Inorg. Chem. **2007**, *46*, 8950–8962

Bifunctional Amine-Tethered Ruthenium(II) Arene Complexes Form Monofunctional Adducts on DNA

Michael Melchart,[†] Abraha Habtemariam,[§] Olga Novakova,[‡] Stephen A. Moggach,[†] Francesca P. A. Fabbiani,[†] Simon Parsons,[†] Viktor Brabec,[‡] and Peter J. Sadler*[,§]

School of Chemistry, University of Edinburgh, West Mains Road, Edinburgh, EH9 3JJ, U.K., Department of Chemistry, University of Warwick, Coventry CV4 7AL, U.K., Institute of Biophysics, Academy of Sciences of the Czech Republic, Kralovopolska 135, 61265 Brno, Czech Republic

Received April 26, 2007

The tethered Ru^{II} half-sandwich complexes $[\eta^6{:}\eta^1\text{-}C_6H_5(CH_2)_nNH_2)RuCl_2]$ **1** ($n = 3$) and **2** ($n = 2$) have been synthesized as potential bifunctional anticancer complexes, and their X-ray crystal structures have been determined. They hydrolyze rapidly in aqueous solution to give predominantly mono-aqua mono-chlorido species. Mono-9EtG adducts, where 9EtG = 9-ethylguanine, form rapidly, but the second 9EtG binds more slowly and more weakly. In the X-ray crystal structure of the di-9EtG adduct $[(\eta^6{:}\eta^1\text{-}C_6H_5(CH_2)_3NH_2)Ru(9EtG)_2](CF_3SO_3)_2{\cdot}H_2O$ (**8**·H_2O), one of the Ru–N7 bonds is significantly longer than the other (2.1588(18) vs 2.101(2) Å). The bound guanine bases adopt a head-to-head configuration, stabilized by tether NH_2 hydrogen bonding to C6O of 9EtG. The X-ray crystal structure of the dinitrato complex $[(\eta^6{:}\eta^1\text{-}C_6H_5(CH_2)_3NH_2)Ru(NO_3)_2]$ (**3**) showed both nitrates to be bound to ruthenium. This complex readily rutheniated calf thymus DNA but failed to produce stop sites on pSP73KB plasmid DNA during DNA transcription by an RNA polymerase. This suggested that only monofunctional DNA adducts formed, as did interstrand cross-linking assays. Also, the unwinding angle induced in negatively supercoiled DNA ($9 \pm 1°$) was less than that induced by cisplatin (13°). These findings may explain why complexes such as **1** and **2** exhibited low cytotoxicities (IC_{50} values >100 μM) toward A2780 human ovarian cancer cells.

Introduction

Metal complexes offer potential as anticancer agents.[1] We have shown that some organometallic Ru^{II} arene complexes of the type $[(\eta^6\text{-arene})Ru(XY)Z]^+$, where XY is a bidentate chelating ligand and Z is a leaving group, can exhibit promising cytotoxicity against various cancer cell lines, including cisplatin-resistant cells.[2,3] Complexes such as $[(\eta^6\text{-arene})Ru(en)Cl]^+$ have one reactive site available and form monofunctional adducts with biomolecules.[4,5] A particularly attractive feature of Ru^{II} arene complexes is the possibility of altering their framework, which provides considerable scope for the optimization of their design, in terms of mechanisms of action, selection of target sites, and modulation of possible side-effects.[6] It is clear from studies so far that the nature of the arene, of the chelating ligand, and of the leaving group can have a major influence on rates of activation (hydrolysis, binding to biomolecules such as DNA bases) as well as activity.[3,7]

It was of interest to explore a different profile of reactivity for ruthenium arene complexes. Structural differences could lead to a different spectrum of activity and increase the scope of this type of complex. Whereas the exact mode of action of cytotoxic ruthenium arene compounds is not known, recent results suggest that DNA may be an important target site

* To whom correspondence should be addressed. E-mail: p.j.sadler@warwick.ac.uk.
[†] University of Edinburgh.
[‡] Institute of Biophysics, Brno.
[§] University of Warwick.

(1) Guo, Z.; Sadler, P. J. *Angew. Chem. Int. Ed.* **1999**, *38*, 1512−1531.
(2) Aird, R. E.; Cummings, J.; Ritchie, A. A.; Muir, M.; Morris, R. E.; Chen, H.; Sadler, P. J.; Jodrell, D. I. *Br. J. Cancer* **2002**, *86*, 1652−1657.
(3) Habtemariam, A.; Melchart, M.; Fernández, R.; Parsons, S.; Oswald, I. D. H.; Parkin, A.; Fabbiani, F. P. A.; Davidson, J. E.; Dawson, A.; Aird, R. E.; Jodrell, D. I.; Sadler, P. J. *J. Med. Chem.* **2006**, *49*, 6858−6868.
(4) Wang, F.; Bella, J.; Parkinson, J. A.; Sadler, P. J. *J. Biol. Inorg. Chem.* **2005**, *10*, 147−155.
(5) Chen, H.; Parkinson, J. A.; Morris, R. E.; Sadler, P. J. *J. Am. Chem. Soc.* **2003**, *125*, 173−186.
(6) Yan, Y. K.; Melchart, M.; Habtemariam, A.; Sadler, P. J. *Chem. Commun.* **2005**, 4764−4776.

10.1021/ic700799w CCC: $37.00
Published on Web 09/13/2007

for $\{(\eta^6\text{-arene})\text{Ru(en)}\}^{2+}$ complexes.[7b] Thus, we are attempting to design ruthenium arene compounds with a variety of potential DNA binding modes. Incorporation of two features into ruthenium arene complexes, which have been closely linked with the mode of action of the anticancer drug cisplatin, appeared particularly attractive. First, cisplatin has two reactive sites available and can bind to its target DNA in a bifunctional manner, forming intra- and interstrand cross-links on DNA.[8] A similar profile of reactivity might be achievable for ruthenium arene complexes because coordination to two guanine bases has been demonstrated for the fragment $\{(\eta^6\text{-benzene})\text{Ru}\}^{2+}$.[9] Second, the activity of platinum am(m)ine anticancer compounds appears to depend on the presence of hydrogen-bond-donating NH groups.[10] Similarly, the critical role of coordinated ligands in Ru^{II} arene complexes in controlling and promoting interactions with DNA nucleobases has been demonstrated.[5,7a,11] For example, in reactions with guanine, cytosine, adenine, and thymine nucleobase derivatives $\{(\eta^6\text{-arene})\text{Ru(en)}\}^{2+}$ react exclusively with guanine derivatives.[5,12] This site-selectivity appears to be controlled by the NH_2 groups of the en ligand, which can form strong hydrogen bonds with the C6O carbonyl group of guanine bases.[13]

Thus, the presence of an hydrogen-bond donor, for example, an amine group, may be an important feature in the design of bifunctional Ru^{II} arene complexes to observe, for example, interstrand cross-links on DNA. Reports in the literature suggest that coordinated monodentate NH_2R ligands in $[(\eta^6\text{-}p\text{-cymene})\text{Ru}(NH_2CMe_3)Cl_2]$ and $[(\eta^6\text{-arene})\text{Ru(L-alaMe)}Cl_2]$ complexes, where L-alaMe = L-alanine methyl ester, can undergo substitution reactions,[14,15] and complexes such as $[(\eta^6\text{-mesitylene})\text{Ru}(NHR_2)Cl_2]$, where R = Et or Bu, decompose in solution.[16] For potential anticancer applications, the chemistry of such complexes might be difficult to predict or control. Stabilization of amine coordination to the ruthenium center can be achieved via chelation. Here, we consider the incorporation of a chelated amine group via a tether to the arene to give a bifunctional Ru^{II} arene complex (Figure 1).

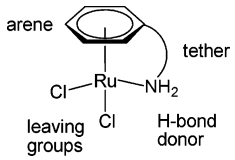

Figure 1. General features of amino-tethered di-chlorido Ru^{II} arene complexes, illustrating the features that might be important for biochemical reactivity.

Research on tethered Ru^{II} arene complexes has received increasing attention over the past few years, mainly due to potential applications in catalysis.[17] Most of the documented examples are bifunctional complexes containing monodentate phosphine ligands and two chloride ligands.[18] Ru^{II} arene complexes containing sulfur[19] and oxygen[20] tethers are also known. At the start of these studies, nitrogen tethers in Ru^{II} arenes had received very little attention. Reported examples include compounds with two[21] or three[22] tethering side-arms, complexes with amine tethers, where either one or both remaining coordination sites on ruthenium are occupied by phosphine ligands or 2,2′-bipyridine respectively,[20,23] and complexes with nitrogen-containing tethered chelating ligands (e.g., $[(\eta^6\text{-}C_6H_5(CH_2)_3NH(1S,2S\text{-}CHC_6H_5)_2NSO_2C_6H_4CH_3\text{-}N,N)\text{RuCl}]$) for use in catalysis.[24] Tethered complexes have mainly been studied in organic solvents.[17a−e,25] In contrast, the emphasis in the present investigations into potential

(7) (a) Fernández, R.; Melchart, M.; Habtemariam, A.; Parsons, S.; Sadler, P. J. *Chem.—Eur. J.* **2004**, *10*, 5173−5179. (b) Wang, F.; Habtemariam, A.; van der Geer, E. P. L.; Fernández, R.; Melchart, M.; Deeth, R. J.; Aird, R.; Guichard, S.; Fabbiani, F. P. A.; Lozano-Casal, P.; Oswald, I. D. H.; Jodrell, D. I.; Parsons, S.; Sadler, P. J. *Proc. Natl. Acad. Sci. U.S.A.* **2005**, *102*, 18269−18274. (c) Dougan, S. J.; Melchart, M.; Habtemariam, A.; Parsons, S.; Sadler, P. J. *Inorg. Chem.* **2006**, *45*, 10882−10894.

(8) (a) Jamieson, E. R.; Lippard, S. J. *Chem. Rev.* **1999**, *99*, 2467−2498. (b) Brabec, V.; Kasparkova, J. *Metal Compounds in Cancer Chemotherapy* **2005**, 187−218. (c) Wang, D.; Lippard, S. J. *Nature Rev. Drug Discovery* **2005**, 4, 307−320.

(9) Korn, S.; Sheldrick, W. S. *J. Chem. Soc., Dalton Trans.* **1997**, 2191−2199.

(10) Reedijk, J. *Chem. Rev.* **1999**, *99*, 2499−2510.

(11) Melchart, M.; Habtemariam, A.; Parsons, S.; Moggach, S. A.; Sadler, P. J. *Inorg. Chim. Acta* **2006**, *359*, 3020−3028.

(12) Morris, R. E.; Aird, R. E.; Murdoch, P. del S.; Chen, H.; Cummings, J.; Hughes, N. D.; Parsons, S.; Parkin, A.; Boyd, G.; Jodrell, D. I.; Sadler, P. J. *J. Med. Chem.* **2001**, *44*, 3616−3621.

(13) Chen, H.; Parkinson, J. A.; Parsons, S.; Coxall, R. A.; Gould, R. O.; Sadler, P. J. *J. Am. Chem. Soc.* **2002**, *124*, 3064−3082.

(14) Sheldrick, W. S.; Heeb, S. *Inorg. Chim. Acta* **1990**, *168*, 93−100.

(15) Bates, R. S.; Begley, M. J.; Wright, A. H.; *Polyhedron* **1990**, *9*, 1113−1118.

(16) Carter, L.; Davies, D. L.; Fawcett, J.; Russell, D. R. *Polyhedron* **1993**, *12*, 1123−1128.

(17) (a) Fürstner, A.; Liebl, M.; Lehmann, C. W.; Picquet, M.; Kunz, R.; Bruneau, C.; Touchard, D.; Dixneuf, P. H. *Chem.—Eur. J.* **2000**, *6*, 1847−1857. (b) Jan, D.; Delaude, L.; Simal, F.; Demonceau, A.; Noels, A. F. *J. Organomet. Chem.* **2000**, *606*, 55−64. (c) Çetinkaya, B.; Demir, S.; Özdemir, I.; Toupet, L.; Esmeril, D.; Bruneau, C.; Dixneuf, P. H. *Chem.—Eur. J.* **2003**, *9*, 2323−2330. (d) Simal, F.; Jan, D.; Demonceau, A.; Noels, A. F. *Tetrahedron Lett.* **1999**, *40*, 1653−1656. (e) Umezawa-Vizzini, K.; Lee, T. R. *Organometallics* **2003**, *22*, 3066−3076. (f) Miyaki, Y.; Onishi, T.; Ogoshi, S.; Kurosawa, H. *J. Organomet. Chem.* **2000**, *616*, 135−139.

(18) (a) Therrien, B.; Ward, T. R.; Pilkington, M.; Hoffmann, C.; Gilardoni, F.; Weber, J. *Organometallics* **1998**, *17*, 330−337. (b) Smith, P. D.; Wright, A. H. *J. Organomet. Chem.* **1998**, *559*, 141−147. (c) Bennett, M. A.; Edwards, A. J.; Harper, J. R.; Khimyak, T.; Willis, A. C. *J. Organomet. Chem.* **2001**, *629*, 7−18. (d) Nelson, J. H.; Ghebreyessus, K. Y.; Cook, V. C. *Organometallics* **2002**, *21*, 1727−1733. (e) Jung, S.; Ilg, K.; Brandt, C. D.; Wolf, J.; Werner, H. *J. Chem. Soc., Dalton Trans.* **2002**, 318−327. (f) Umezawa-Vizzini, K.; Guzman-Jimenez, I. Y.; Whitmire, K. H.; Lee, T. R. *Organometallics* **2003**, *22*, 3059−3065.

(19) Bennett, M. A.; Goh, L. Y.; Willis, A. C. *J. Am. Chem. Soc.* **1996**, *118*, 4984−4992.

(20) (a) Miyaki, Y.; Onishi, T.; Kurosawa, H. *Inorg. Chim. Acta* **2000**, *300*−302, 369−377. (b) Soleimannejad, J.; Sisson, A.; White, C. *Inorg. Chim. Acta* **2003**, *352*, 121−128. (c) Kitaura, R.; Miyaki, Y.; Onishi, T.; Kurosawa, H. *Inorg. Chim. Acta* **2002**, *334*, 142−148. (d) Èubrilo, J.; Hartenbach, I.; Schleid, T.; Winter, R. F. *Z. Anorg. Allg. Chem.* **2006**, *632*, 400−408.

(21) (a) Therrien, B.; Ward T. R. *Angew. Chem. Int. Ed.* **1999**, *38*, 405−408. (b) Therrien, B.; König, A.; Ward, T. R. *Organometallics* **1999**, *18*, 1565−1568.

(22) (a) Hartshorn, C. M.; Steel, P. J. *Aust. J. Chem.* **1995**, *48*, 1587−1599. (b) Hartshorn, C. M.; Steel, P. J. *Angew. Chem., Int. Ed. Engl.* **1996**, *35*, 2655−2657. (c) Sun, W. Y.; Xie, J.; Okamura, T.; Huang, C. K.; Ueyama, N. *Chem. Commun.* **2000**, 1429−1430.

(23) Scolaro, C.; Geldbach, T. J.; Rochat, S.; Dorcier, A.; Gossens, C.; Bergamo, A.; Cocchietto, M.; Tavernelli, I.; Sava, G.; Rothlisberger, U.; Dyson, P. J. *Organometallics* **2006**, *25*, 756−765.

(24) (a) Cheung, F. K.; Hayes, A. M.; Hannedouche, J.; Yim, A. S. Y.; Wills, M. *J. Org. Chem.* **2005**, *70*, 3188−3197. (b) Hayes, A. M.; Morris, D. J.; Clarkson, G. J.; Wills, M. *J. Am. Chem. Soc.* **2005**, *127*, 7318−7319.

bifunctional amine-tethered ruthenium arene complexes for anticancer applications is on studies in aqueous media.

In this article, we describe the synthesis and characterization, both in solution and in the solid state, of water-soluble bifunctional amine-tethered Ru^{II} arene complexes.[26] We have studied their hydrolysis behavior and have investigated their interactions with the DNA model base 9-ethylguanine (9EtG), both in solution and by X-ray crystallography. The studies are complemented by biophysical experiments using plasmid DNA, and the data are discussed in relation to the observed lack of biological activity.

Experimental Section

Materials. The ruthenium dimer precursor $[(\eta^6\text{-etb})RuCl_2]_2$, where etb = ethyl benzoate, was prepared according to a previously published route (also, see Supporting Information).[18a] Most reagents were obtained from Aldrich, including D_2O (99.9%) and $CDCl_3$ (99.8%). Nucleobase derivatives were acquired from Sigma Aldrich. Most solvents, as well as silver nitrate and sodium chloride, were supplied by Fisher. Ethanol was dried over Mg/I_2. 1,4-Dioxane was supplied by Rathburn, 1,2-dichloroethane was obtained from both Prolabo and Aldrich, and $RuCl_3 \cdot xH_2O$ from Alfa Aesar. *cis*-Diamminedichloridoplatinum(II) (cisplatin) and *trans*-diamminedichloridoplatinum(II) (transplatin) were purchased from Sigma (Prague). Chlorodiethylenetriamineplatinum(II) chloride, [Pt(dien)Cl]Cl, was a kind gift of Professor Giovanni Natile from the University of Bari.

Stock solutions (5×10^{-4} M) of **3** and platinum complexes for use in DNA studies were prepared in the dark at 298 K. Calf thymus (CT) DNA (42% guanine + cytosine, mean molecular mass ca. 2×10^7) was also prepared and characterized as described previously.[27,28] Plasmids pSP73KB and pSP73 (2455 and 2464 bp, respectively)[29] were isolated according to standard procedures and banded twice in CsCl/EtBr equilibrium density gradients. Restriction endonucleases were purchased from New England Biolabs (Beverly, MA). Riboprobe Gemini System II for transcription mapping containing SP6 and T7 RNA polymerases was purchased from Promega (Madison, WI). Ethidium bromide (EtBr) and agarose were from Merck KgaA (Darmstadt, Germany). The radioactive products were obtained from Amersham (Arlington Heights, IL).

Preparations. $[(\eta^6\text{:}\eta^1\text{-}C_6H_5(CH_2)_3NH_2)RuCl_2]$ (1). $[(\eta^6\text{-etb})RuCl_2]_2$ (372.4 mg, 0.58 mmol) and 3-phenyl-1-propylamine (148.5 mg, 1.10 mmol) were dissolved in 1,2-dichloroethane (50 mL). A few drops of THF were added, the solution was stirred for 60 min, and then was heated to reflux for 90 h under argon. The solvent was removed on a rotary evaporator, and the product was extracted with methanol, which was concentrated on a rotary evaporator until precipitation of the product occurred. Diethyl ether was added, and the solution was stored at 253 K overnight. The yellow-orange microcrystalline solid (129.2 mg, 0.42 mmol, 42.1% yield) was collected by filtration, washed with diethyl ether, and dried in air. ^{1}H NMR ($CDCl_3$): δ 5.88 (t, 2H, $J = 6$ Hz), 5.73 (t, 1H, $J = 6$ Hz), 5.16 (d, 2H, $J = 6$ Hz), 3.22 (b, 2H), 2.95 (m, 2H, $J = 5.5$ Hz), 2.49 (t, 2H, $J = 6$ Hz), 2.20 (m, 2H). Elemental analysis: Calcd for $C_9H_{13}NRuCl_2$: C, 35.19; H, 4.27; N, 4.56. Found: C, 35.45; H, 3.85; N, 4.51. Crystals of **1**, suitable for X-ray diffraction, were obtained from a methanol solution at 253 K.

$[(\eta^6\text{:}\eta^1\text{-}C_6H_5(CH_2)_2NH_2)RuCl_2]$ (2). $[(\eta^6\text{-etb})RuCl_2]_2$ (420.5 mg, 0.65 mmol) and 2-phenethylamine (150.0 mg, 1.24 mmol) were dissolved in 1,2-dichloroethane (50 mL). A few drops of THF were added, the solution was stirred for 60 min, and then was heated to reflux for 41 h under argon. The solvent was removed on a rotary evaporator, and the product was extracted with methanol, which was concentrated on a rotary evaporator until precipitation occurred. Diethyl ether was added, and the solution was stored at 253 K for 2 d. The orange microcrystalline solid (182.8 mg, 0.62 mmol, 50.4% yield) was collected by filtration, washed with diethyl ether, and dried in air. ^{1}H NMR ($CDCl_3$): δ 5.94 (t, 2H, $J = 5.5$ Hz), 5.53 (t, 1H, $J = 5.5$ Hz), 5.22 (d, 2H, $J = 5.5$ Hz), 3.90 (m, 2H, $J = 5.5$ Hz), 3.60 (b, 2H), 2.84 (m, 2H, $J = 6.5$ Hz). Elemental analysis: Calcd for $C_8H_{11}NRuCl_2$: C, 32.78; H, 3.78; N, 4.78. Found: C, 33.08; H, 3.83; N, 4.76. Crystals of **2**, suitable for X-ray diffraction, were grown from water, after the addition of NaCl, at ambient temperature.

$[(\eta^6\text{:}\eta^1\text{-}C_6H_5(CH_2)_3NH_2)Ru(NO_3)_2]$ (3). Complex **1** (110.3 mg, 0.36 mmol) and silver nitrate (121.9 mg, 0.72 mmol) were dissolved in water (25 mL), and the solution was stirred for 150 min. After filtration, the solvent was removed on a rotary evaporator, and the product was extracted with water. Filtration and removal of the solvent on a rotary evaporator yielded an orange powder (121.5 mg, 0.34 mmol, 93.9% yield), which was collected by filtration, washed with diethyl ether, and dried in air. ^{1}H NMR (90% H_2O/10% D_2O, pH 4.10): δ 6.07 − 6.02 (m, 3H), 5.43 (d, 2H, $J = 6$ Hz), 3.96 (b, 2H), 2.97 (m, 2H), 2.57 (t, 2H, $J = 6$ Hz), 2.30 (m, 2H). X-ray diffraction quality crystals of **3** were obtained by slow diffusion of diethyl ether into an acetone solution of **3** at ambient temperature.

$[(\eta^6\text{:}\eta^1\text{-}C_6H_5(CH_2)_3NH_2)Ru(9EtG)_2](NO_3)_{0.25}(PF_6)_{1.75}$ (7). **3** (43.8 mg, 122 μmol) and 9EtG (47.2 mg, 264 μmol) were dissolved in methanol (15 mL), and the mixture was stirred for 20 h. The solution was concentrated to ca. 5 mL on a rotary evaporator and heated to dissolve the greenish precipitate. Addition of NH_4PF_6 (177.5 mg, 1.09 mmol) was followed by addition of diethyl ether, which led to the formation of a greenish precipitate, and the solution was stored at ambient temperature overnight. The light-green powder (98.1 mg) was collected by filtration, washed with diethyl ether, and dried in air. ^{1}H NMR (D_2O, pH meter reading pH* 6.56): δ 8.25 (s, 1H), 5.88 (t, 2H, $J = 6$ Hz), 5.81 (t, 1H, $J = 6$ Hz), 5.79 (d, 2H, $J = 6$ Hz), 5.42 (m, 1H), 4.17−4.03 (m, 4H), 2.73 (m, 2H), 2.65 (m, 2H), 2.32 (m, 2H), 1.33 (t, 3H, $J = 7$ Hz). Crystals of $[(\eta^6\text{:}\eta^1\text{-}C_6H_5(CH_2)_3NH_2)Ru(9EtG)_2](NO_3)_2$ (**6A**), which diffracted poorly, were grown by slow evaporation of an acetone solution containing **7** at ambient temperature. Elemental analysis: Calcd for $C_{23}H_{31}N_{11.25}O_{2.75}RuP_{1.75}F_{10.5}$: C, 31.98; H, 3.62; N, 18.24. Found: C, 31.94; H, 3.57; N, 18.55.

$[(\eta^6\text{:}\eta^1\text{-}C_6H_5(CH_2)_3NH_2)Ru(9EtG)_2](CF_3SO_3)_2$ (8). **1** (37.9 mg, 123 μmol) and 9EtG (51.4 mg, 287 μmol) were dissolved in methanol (25 mL), and the mixture was stirred for 22 h. The solution was concentrated to ca. 10 mL on a rotary evaporator and $NaCF_3SO_3$ (176.3 mg, 1.02 mmol) was added. The solvent was removed on a rotary evaporator, and the product was extracted with acetone. The solution was filtered, the solvent was removed on a rotary evaporator, and a yellow-green powder (228.4 mg) was collected, washed with diethyl ether, and dried in air. The powder was washed with a minimal amount of ethanol to dissolve the excess $NaCF_3SO_3$. The solution was filtered, and the yellow powder was

(25) (a) Faller, J. W.; D'Alliessi, D. G. *Organometallics* **2003**, *22*, 2749−2757. (b) Faller, J. W.; Fontaine, P. P. *Organometallics* **2005**, *24*, 4132−4138.
(26) Presented in part at the First European Conference on Chemistry for Life Sciences, Rimini, Italy, 4−8 October, 2005. Abstract p 148.
(27) Brabec, V.; Palecek, E. *Biophysik* **1970**, *6*, 290−300.
(28) Brabec, V.; Palecek, E. *Biophys. Chem.* **1976**, *4*, 76−92.
(29) Lemaire, M. A.; Schwartz, A.; Rahmouni, A. R.; Leng, M. *Proc. Natl. Acad. Sci. U.S.A.* **1991**, *88*, 1982−1985.

then washed with diethyl ether. X-ray diffraction quality crystals were obtained as **8**·H_2O by diffusion of diethyl ether into an acetone solution of **8** at ambient temperature.

Methods and Instrumentation. (a) X-ray Crystallography. All of the diffraction data were collected using a Bruker Smart Apex CCD diffractometer equipped with an Oxford Cryosystems low-temperature device operating at 150 K. Absorption corrections for all of the data sets were performed with the multiscan procedure *SADABS*.[30] Structures were solved using direct methods (*SHELXS*[31] or *SIR92*[32]) or Patterson methods (*DIRDIF*).[33] Complexes were refined against F^2 using *CRYSTALS*[34] (**1** and **4**) or *SHELXL* (**2** and **3**).[35] Hydrogen atoms were placed in idealized positions. The crystal of **1** was twinned via a 2-fold rotation about the [100] direct lattice direction; the twin scale factor was 0.477(5). The tether is also disordered over two conformations. The structure is very close to being in *Pnma*; however, reflections that would have been absent for the *n* and 2_1 symmetry elements were clearly stronger than the absences corresponding to the genuine glide. In **2**, one carbon atom of the tether is disordered about a crystallographic mirror plane. In **4**, one terminal methyl group of one of the 9EtG ligands is disordered over two positions. Disordered acetone of crystallization was treated with the van der Sluis−Spek procedure.[36] X-ray crystallographic data for complexes **1**−**4** are available in the Supporting Information and have been deposited in the CCDC under accession numbers 639637−639640, respectively.

(b) NMR Spectroscopy. ^{1}H NMR spectra were acquired for samples in 5 mm NMR tubes at 298 K (unless stated otherwise) on either a Bruker DMX 500 or a Bruker AVA 600 NMR spectrometer, using TBI [^{1}H, ^{13}C, X] or TXI [^{1}H, ^{13}C, X] probeheads equipped with *z*-field gradients. All of the data processing was carried out using *XWIN-NMR* version 3.6 (Bruker U.K. Ltd.). ^{1}H NMR chemical shifts were internally referenced to TSP or TMS via 1,4-dioxane (3.75 ppm) or C*H*Cl_3 (7.27 ppm).

1D and 2D spectra were recorded using standard pulse sequences, which were modified by Dr. Dusan Uhrin and Mr. Juraj Bella, at the University of Edinburgh. Water signals were suppressed using Presaturation or Shaka methods.[37]

In time-course ^{1}H NMR experiments, the time of dissolution of the reactants, or when solutions of all of the reactants were mixed, is taken as $t = 0$ min.

(c) pH Measurements. The pH values of NMR solutions were measured at ambient temperature directly in the NMR tube, before and after recording NMR spectra, using a Corning 145 pH meter equipped with an Aldrich micro combination electrode calibrated with Aldrich buffer solutions at pH 4, 7, and 10. The pH values were adjusted with dilute $HClO_4$ and NaOH. No correction has been applied for the effect of deuterium on the glass electrode. For measurements in D_2O, pH* = pH meter reading of the solution.

(d) CHN Analysis. CHN elemental analysis was performed by the CHN service at the University of St Andrews.

(e) Chloride Titrations. Chloride was added to the NMR samples as aliquots of a 3 M solution of sodium chloride. $[Cl^-]_t$ refers to the concentration of total chloride in solution. The amount of bound chloride was calculated from the relative proportions of the signals for the di-chlorido, the mono-aqua and the di-aqua species by integration. Hydrolysis equilibrium constants were calculated using the following equations. $K_1 = ([Ru(Cl)H_2O] * [Cl^-]_f)/[RuCl_2]$ and $K_2 = ([Ru(H_2O)_2] * [Cl^-]_f)/[Ru(Cl)H_2O]$, where $[Cl^-]_f$ = the concentration of free chloride in solution.

(f) Time-Course of Reactions with 9EtG. All of the experiments were carried out in 90% H_2O/10% D_2O at 298 K, unless stated otherwise. Reactants were added to 5 mm NMR tubes, which contained 600 μL of a 2.2 mM solution of 9EtG and 5 μL of a 1% solution of 1,4-dioxane.

[(η^6:η^1-$C_6H_5(CH_2)_3NH_2$)Ru(NO_3)$_2$] (3). A 58.4 μL aliquot of a 12.9 mM solution of **3** was added to the NMR tube, and the pH of the solution was measured (5.19). ^{1}H NMR spectra were recorded at $t = 24$ min, $t = 46$ min, and then every 20 min from $t = 46$ min for a period of 16.5 h. The pH of the solution after 16.5 h was 6.22.

[(η^6:η^1-$C_6H_5(CH_2)_3NH_2$)$RuCl_2$] (1) in the presence of chloride ($[Cl^-]_t$ = 21.7 mM). A 4.4 μL aliquot of a 3 M solution of NaCl was added to the NMR tube, followed by 58.4 μL of a 11.3 mM solution of **1**, and the pH of the solution was measured (6.08). ^{1}H NMR spectra were recorded at $t = 45$ min, and five times between $t = 45-134$ min, and then every 30 min from $t = 134$ min for a period of 18 h. The pH of the solution after 18 h was 6.53.

[(η^6:η^1-$C_6H_5(CH_2)_2NH_2$)$RuCl_2$] (2) in the presence of chloride ($[Cl^-]_t$ = 21.7 mM). A 4.4 μL aliquot of a 3 M solution of NaCl was added to the NMR tube, followed by 58.4 μL of a 11.3 mM solution of **2**, and the pH of the solution was measured (6.08). ^{1}H NMR spectra were recorded at $t = 32$ min, $t = 53$ min, and then every 30 min from $t = 123$ min for a period of 41 h. The pH of the solution after 41 h was 6.23.

Hydrolysis of [(η^6:η^1-$C_6H_5(CH_2)_3NH_2$)Ru(9EtG)$_2$]$^{2+}$. The ^{1}H NMR spectrum of a solution of [(η^6:η^1-$C_6H_5(CH_2)_3NH_2$)Ru(9EtG)$_2$]-$(NO_3)_{0.25}(PF_6)_{1.75}$ (**7**) (3.0 mM) in D_2O at pH* 6.67 was recorded at $t = 10$ min, $t = 19$ min, and then every 20 min from $t = 42$ min for a period of 20 h. The pH* of the solution after 20 h was 6.02.

(g) DNA Metalation Reactions. Solutions of double-helical CT DNA and plasmid DNA at a concentration of 0.1 mg/mL were incubated with **3** or platinum complex in 10 mM $NaClO_4$ (pH ~6) at 310 K for 24 h in the dark, at the r_i value of 0.1 (r_i is defined as the molar ratio of metal complex to nucleotide phosphates at the onset of incubation with DNA). At various time intervals, an aliquot of the reaction mixture was withdrawn, quickly cooled on an ice bath, precipitated by ethanol, and the content of ruthenium (or platinum) in the supernatant of these samples was determined by flameless atomic absorption spectrophotometry (FAAS), thus allowing determination of the number of atoms of the metal bound per nucleotide residue (r_b values).[38] The binding of the ruthenium compounds to CT DNA was also quantified in a different way. Aliquots of the reaction mixture withdrawn at various time intervals were quickly cooled on an ice bath and filtered using Sephadex G50 to remove free (unbound) ruthenium compound. The content

(30) Sheldrick, G. M. *SADABS Version 2006−1*; University of Göttingen, Göttingen, Germany, 2006.
(31) Sheldrick, G. M. *SHELXS-97*, University of Göttingen, Göttingen, Germany, 1997.
(32) Altomare, A.; Cascarano, G.; Giacovazzo, C.; Guagliardi, A.; Burla, M. C.; Polidori, G.; Camalli, M. *SIR92*: A Program for Automatic Solution of Crystal Structures by Direct Methods, *J. Appl. Cryst.* **1994**, *27*, 435−435.
(33) Beurskens, P. T.; Beurskens, G.; Bosman, W. P.; de Gelder, R.; Garcia-Granda, S.; Gould, R. O.; Israel, R.; Smits, J. M. M. *The DIRDIF96 Program System*, University of Nijmegen: Nijmegen, The Netherlands, 1996.
(34) Betteridge, P. W.; Carruthers, J. R.; Cooper, R. I.; Prout, K.; Watkin, D. J. *CRYSTALS*, version 12: software for guided crystal structure analysis, *J. Appl. Cryst.* **2003**, *36*, 1487.
(35) Sheldrick, G. M. *SHELXL-97*, University of Göttingen: Göttingen, Germany, 1997.
(36) van der Sluis, P.; Spek, A. L. *BYPASS*: An Effective Method for the Refinement of Crystal Structures Containing Disordered Solvent Regions. *Acta Crystallographica, Section A* **1990**, *46*, 194−201.
(37) Hwang, T. L.; Shaka, A. J. *J. Magn. Reson.* **1995**, *Series A 112*, 275−279.
(38) Malina, J.; Novakova, O.; Keppler, B. K.; Alessio, E.; Brabec, V. *J. Biol. Inorg. Chem.* **2001**, *6*, 435−445.

of ruthenium in these DNA samples was determined by FAAS. Results identical to those obtained using the assay based on DNA precipitation by ethanol were obtained.

(h) DNA Transcription by RNA Polymerase In Vitro. Transcription of the (*Nde*I/*Hpa*I) restriction fragment of pSP73KB DNA with T7 RNA polymerase and electrophoretic analysis of transcripts were performed according to the protocols recommended by Promega (Promega Protocols and Applications, 43−46 (1989/90) and previously described in detail.[29,39]

(i) DNA Interstrand Crosslinking Assay. Complex **3** or cisplatin were incubated with 1 μg of pSP73 DNA linearized by *Eco*RI at various r_b values (0.001−0.01). The metalated samples were precipitated by ethanol and analyzed for DNA interstrand cross-links, in the same way as described recently.[39,40] The linear duplexes were first 3′-end labeled using a Klenow fragment of DNA polymerase I in the presence of [α-^{32}P]dATP. The samples were deproteinized by phenol, precipitated by ethanol, and the pellet was dissolved in 18 μL of a solution containing 30 mM NaOH, 1 mM EDTA, 6.6% sucrose, and 0.04% bromophenol blue. The amount of interstrand cross-links was analyzed by electrophoresis under denaturing conditions on an alkaline agarose gel (1%). After the electrophoresis was completed, the intensities of the bands corresponding to single strands of DNA and interstrand cross-linked duplex were quantified. The radioactivity associated with the individual bands in each lane was measured to obtain estimates of the fraction of noncross-linked or cross-linked DNA under each condition. The frequency of interstrand cross-links (%ICL per platinum) was calculated using the Poisson distribution from the fraction of noncross-linked DNA, in combination with the r_b values and the fragment size.

(j) Unwinding of Negatively Supercoiled DNA. Unwinding of closed circular supercoiled pSP73KB plasmid DNA was assayed by an agarose gel mobility shift assay.[41] The unwinding angle μ induced per metal−DNA adduct was calculated upon the determination of the r_b value at which the complete transformation of the supercoiled to relaxed form of the plasmid was attained. Samples of pSP73KB plasmid were incubated with **3** or cisplatin in 10 mM $NaClO_4$ at 310 K in the dark for 24 h. All of the samples were precipitated by ethanol and redissolved in 10 mM $NaClO_4$. An aliquot of the precipitated sample was subjected to electrophoresis on 1% agarose gels, running at 298 K in the dark with TAE buffer (0.04 M tris-acetate + 1 mM EDTA, pH 7.0) with the voltage set at 30 V. The gels were then stained with EtBr, followed by photography on Polaroid 667 film with a transilluminator. The other aliquot was used for the determination of r_b values by FAAS.

(k) Other Methods. Absorption spectra were measured with a Beckmann DU-7400 spectrophotometer. FAAS measurements were carried out with a Varian AA240Z Zeeman atomic absorption spectrometer equipped with a GTA 120 graphite tube atomizer. The gels were visualized using a BAS 2500 FUJIFILM bioimaging analyzer, and the radioactivities associated with bands were quantitated with the AIDA image analyzer software (Raytest, Germany).

(l) Cytotoxicity. Complexes **1** and **2** were tested against the A2780 human ovarian cancer cell line, according to a previously published protocol.[3]

Chart 1. Tethered Ruthenium Arene Complexes Studied in This Work

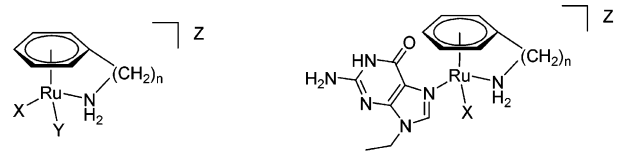

	n	X	Y	Z
1	3	Cl	Cl	
1A	3	Cl	H_2O	Cl
1B	3	H_2O	H_2O	2Cl
2	2	Cl	Cl	
2A	2	Cl	H_2O	Cl
2B	2	H_2O	H_2O	2Cl
3	3	NO_3	NO_3	
3A	3	H_2O	H_2O	$2NO_3$

	n	X	Z
4	3	Cl	Cl
4A	3	H_2O	2Cl
4B	3	9EtG	2Cl
5	2	Cl	Cl
5A	2	H_2O	2Cl
5B	2	9EtG	2Cl
6	3	H_2O	$2NO_3$
6A	3	9EtG	$2NO_3$
7	3	9EtG	$(NO_3)_{0.25}(PF_6)_{1.75}$
7A		H_2O	$(NO_3)_{0.25}(PF_6)_{1.75}$
8	3	9EtG	$2CF_3SO_3$

Results

Synthesis and Characterization. The precursor diene ethyl-1,4-cyclohexadiene-3-carboxylate for the synthesis of ruthenium dimer $[(\eta^6\text{-etb})RuCl_2]_2$ was synthesized via the Birch reduction of benzoic acid, followed by esterification, because the direct reduction of ethyl benzoate[42] gave rise to mainly benzoic acid under the reported conditions (Chart S1).

The syntheses of $[(\eta^6{:}\eta^1\text{-}C_6H_5(CH_2)_3NH_2)RuCl_2]$ (**1**) and $[(\eta^6{:}\eta^1\text{-}C_6H_5(CH_2)_2NH_2)RuCl_2]$ (**2**) (Chart 1) were based on the route employed by Ward et al.[18a] and involve the thermal displacement of ethyl benzoate (etb) from $[(\eta^6\text{-etb})RuCl_2]_2$ by the appropriate nitrogen-donor derivative (Chart S2). Reactions of $[(\eta^6\text{-etb})RuCl_2]_2$ with either 3-phenyl-1-propylamine or 2-phenethylamine in 1,2-dichloroethane heated under reflux and an argon atmosphere resulted in **1** and **2**, respectively, with satisfactory yields and purity.

The complexes were characterized by CHN elemental analysis and ^{1}H NMR spectroscopy. The arene ^{1}H NMR signals (triplet, triplet, doublet in a 2:1:2 ratio) for the amine-tethered complexes **1** and **2** are shifted to high field by ca. 1.4−2.0 ppm compared to those of the respective free ligands. The signals for the bound NH_2 groups are shifted to low field by 1.9−2.2 ppm compared to the free ligand. The chemical shifts of the CH_2 groups of the tether are also shifted by coordination to ruthenium by as much as 0.9 ppm to low field for the CH_2 group adjacent to the amine in **2**. For **1**, the shift changes for the tether CH_2 peaks range from 0.2 ppm to high field to 0.4 ppm to low field upon the coordination of the tether. Assignment of the CH_2 peaks was aided by the coupling of the CH_2 protons to the amine protons. This was not observed for the free ligands. The assignment of peaks was confirmed for complex **1** by a 2D NOESY spectrum (Figure S1).

The synthesis of di-aqua complex $[(\eta^6{:}\eta^1\text{-}C_6H_5(CH_2)_3NH_2)Ru(H_2O)_2](NO_3)_2$ (**3A**) was attempted by abstraction of the chloride ligands from $[(\eta^6{:}\eta^1\text{-}C_6H_5(CH_2)_3NH_2)RuCl_2]$ (**1**) with silver nitrate in water. The complex, however, crystal-

(39) Brabec, V.; Leng, M. *Proc. Natl. Acad. Sci. U.S.A.* **1993**, *90*, 5345−5349.
(40) Farrell, N.; Qu, Y.; Feng, L.; Van Houten, B. *Biochemistry* **1990**, *29*, 9522−9531.
(41) Keck, M. V.; Lippard, S. J. *J. Am. Chem. Soc.* **1992**, *114*, 3386−3390.
(42) Rabideau, P. W.; Huser, D. L.; Nyikos, S. J. *Tetrahedron Lett.* **1980**, *21*, 1401−1404.

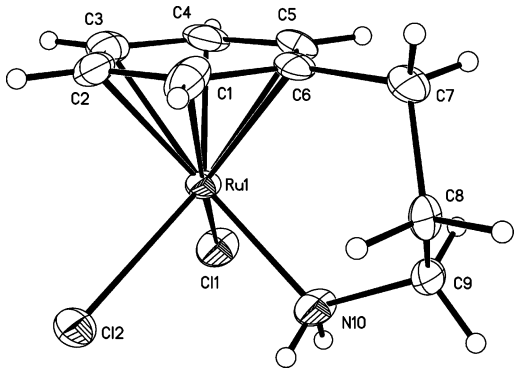

Figure 2. Ortep diagram (50% probability ellipsoids) and atom numbering scheme for the X-ray crystal structure of [(η^6:η^1-$C_6H_5(CH_2)_3NH_2$)$RuCl_2$] (**1**). The tether is disordered, and the alternative conformation is shown in Figure S2.

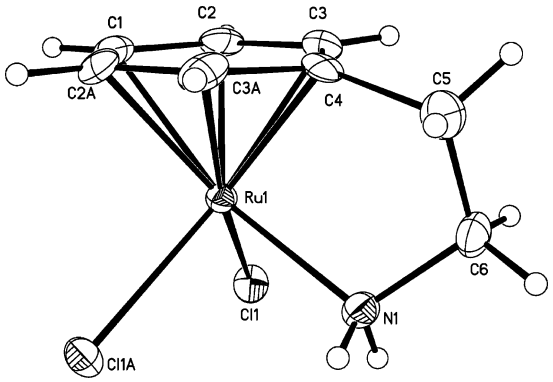

Figure 3. Ortep diagram (50% probability ellipsoids) and atom numbering scheme for the X-ray crystal structure of [(η^6:η^1-$C_6H_5(CH_2)_2NH_2$)$RuCl_2$] (**2**). The tether is disordered, and the alternative conformation is shown in Figure S3.

lized as the dinitrato adduct [(η^1:η^6-$C_6H_5(CH_2)_3NH_2$)Ru-$(NO_3)_2$] (**3**) (vide infra) rather than as the nitrate salt of the di-aqua adduct.

The di-9EtG adduct [(η^6:η^1-$C_6H_5(CH_2)_3NH_2$)Ru(9EtG)$_2$]-$(NO_3)_{0.25}(PF_6)_{1.75}$ (**7**) was synthesized by the reaction of complex **3** with 2.2 mol equiv of 9EtG. Addition of NH_4-PF_6 resulted in a complex with mixed counteranions according to CHN analysis. [(η^6:η^1-$C_6H_5(CH_2)_3NH_2$)Ru(9EtG)$_2$]-$(CF_3SO_3)_2$ (**8**) was synthesized similarly to **7** starting from complex **1**.

X-ray Crystal Structures. In the structure of amine-tethered complex [(η^6:η^1-$C_6H_5(CH_2)_3NH_2$)$RuCl_2$] (**1**), the three-carbon tether adopts two orientations due to disorder (Figures 2 and S2). The crystal data are shown in Table S1 and bond angles and lengths in Table S3. The Ru−Cl bond lengths are 2.425(3) and 2.437(3) Å, and the Ru−N distance is 2.129(5) Å. The Ru−C(arene) bond lengths in **1** are in the range of 2.161(9)−2.196(7) Å, and the Ru−centroid distance is 1.65 Å. The Ru−C6−C7 angle, where C6 is the arene carbon connected to the tether and C7 is the first carbon atom of the tether, is 127.17°. The angle between the plane defined by the arene carbons and that containing C6, Ru, and N is 88.77°.

Complex [(η^6:η^1-$C_6H_5(CH_2)_2NH_2$)$RuCl_2$] (**2**), which contains two carbon atoms in the tether backbone, crystallized with the tether disordered over two positions, similar to **1**, and contains a mirror plane through atoms C4, C1, C5, Ru, and N1 (Figures 3 and S3). The crystal data are shown in Table S1 and bond angles and lengths in Table S4. The Ru−Cl bond lengths are 2.4133(7) Å, and the Ru−N distance is 2.117(3) Å. The Ru−C(arene) bond lengths are in the range of 2.095(3)−2.199(4) Å, and the Ru−centroid distance is 1.63 Å. The arene carbon C4 (to which the tether is connected) is displaced toward the ruthenium center by 0.0733 Å, with respect to the plane defined by carbon atoms C2 and C3, whereas the opposite carbon C1 is the furthest away from the metal (by 0.0066 Å, with respect to the plane defined by carbon atoms C2 and C3) resulting in buckling of the arene ring. The Ru−C4−C5 angle, where C5 is the first carbon atom of the tether, is 114.74°. The angle between the plane defined by the arene carbons and that containing C4, Ru, and N is 90.00°.

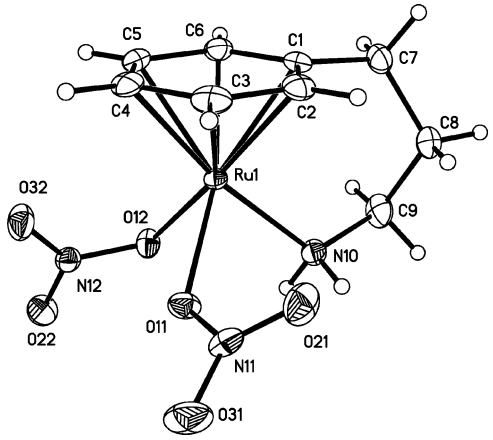

Figure 4. Ortep diagram (50% probability ellipsoids) and atom numbering scheme for the X-ray crystal structure of [(η^6:η^1-$C_6H_5(CH_2)_3NH_2$)Ru$(NO_3)_2$] (**3**).

The X-ray crystal structure of [(η^1:η^6-$C_6H_5(CH_2)_3NH_2$)-Ru$(NO_3)_2$] (**3**) is shown in Figure 4, and the crystal data are listed in Table S2 and bond angles and lengths in Table S5. The Ru−O bond lengths are 2.1172(10) and 2.1250(10) Å, and the Ru−N distance is 2.1241(13) Å. The Ru−C(arene) bond lengths are in the range of 2.1697(15)−2.1986(17) Å, and the Ru−centroid distance is 1.66 Å. Strong hydrogen bonds between the amine protons and oxygen atoms of the nitrate ligands result in the formation of dimers (Figure S4). The angle between the plane defined by the arene carbons and that containing C1 (to which the tether is connected) Ru, and N(tether) is 83.96°.

The X-ray crystal structure of [(η^1:η^6-$C_6H_5(CH_2)_3NH_2$)-Ru(9EtG)$_2$]$(NO_3)_2$ (**6A**), obtained from an acetone solution containing [(η^6:η^1-$C_6H_5(CH_2)_3NH_2$)Ru(9EtG)$_2$]$(NO_3)_{0.25}$-$(PF_6)_{1.75}$ (**7**), was not fully refined because the crystals were of poor quality (Figure S5). However, good quality crystals of the triflate salt [(η^6:η^1-$C_6H_5(CH_2)_3NH_2$)Ru(9EtG)$_2$]$(CF_3$-$SO_3)_2$·H_2O (**8**·H_2O) were obtained. The structure is shown in Figure 5, and the crystal data are listed in Table S2 and bond angles and lengths in Table 1. The Ru−N(tether) bond length is 2.121(2) Å, and the Ru−N(9EtG) distances are 2.101(2) and 2.1588(18) Å, respectively. The Ru−C(arene) bond lengths are between 2.165(2)−2.232(3) Å, and the Ru−centroid distance is 1.67 Å. The angle between the plane

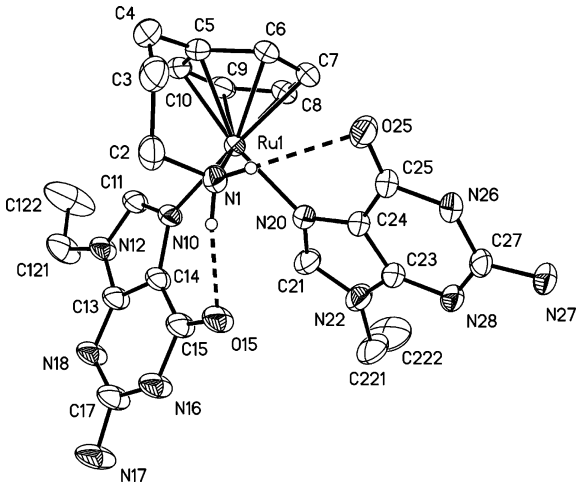

Figure 5. Ortep diagram (50% probability ellipsoids) and atom numbering scheme for the cation in the X-ray crystal structure of $[(\eta^6{:}\eta^1\text{-}C_6H_5(CH_2)_3NH_2)Ru(9EtG)_2](CF_3SO_3)_2{\cdot}H_2O$ (**8**·H_2O). The hydrogen atoms, with the exception of the tether NH_2 protons, have been omitted for clarity. Both of the tether amine protons show intramolecular hydrogen bonds with the carbonyl groups of the two 9EtG ligands, where H11···O15 = 1.98 Å (N1···O15 = 2.869(3) Å) and H12···O25 = 2.32 Å (N1···O25 = 3.085(3) Å).

Table 1. Selected Bond Lengths (Angstroms) and Angles (Degrees) for $[(\eta^6{:}\eta^1\text{-}C_6H_5(CH_2)_3NH_2)Ru(9EtG)_2](CF_3SO_3)_2{\cdot}H_2O$ (**8**·H_2O)

bond	length	bond	length/angle
Ru−N1	2.121(2)	Ru−C10	2.191(2)
Ru−N10	2.1588(18)	Ru−centroid	1.6718(11)
Ru−N20	2.101(2)	N1−Ru−N10	86.94(8)
Ru−C5	2.178(2)	N1−Ru−N20	82.96(8)
Ru−C6	2.172(2)	N10−Ru−N20	87.49(8)
Ru−C7	2.165(2)	Ru−N1−C2	117.26(17)
Ru−C8	2.210(3)	Ru−C5−C4	123.85(19)
Ru−C9	2.232(3)	N1−Ru−C5	89.94(10)

defined by all of the arene carbons and that of C5 (to which the tether is connected), Ru, and N(tether) is 72.77°. The coordinated 9EtG ligands show a number of hydrogen-bond interactions with the tether amine, residual solvent water, the CF_3SO_3 counteranion, and neighboring 9EtG ligands (Figure S6). Both the tether amine protons are involved in intramolecular hydrogen bonds of 1.98 and 2.32 Å, with the carbonyl groups of the two 9EtG ligands.

Aqueous Chemistry. Di-chlorido tethered complexes $[(\eta^6{:}\eta^1\text{-}C_6H_5(CH_2)_3NH_2)RuCl_2]$ (**1**) and $[(\eta^6{:}\eta^1\text{-}C_6H_5(CH_2)_2NH_2)RuCl_2]$ (**2**) have good aqueous solubility. Solutions of **1** (7.2 mM, pH* 5.66) and **2** (7.0 mM Ru, pH* 5.60) in D_2O at 298 K showed no evidence of decomposition over a period of 24 h, as judged by ^{1}H NMR spectroscopy.

Upon dissolution of **1** in D_2O, the ^{1}H NMR spectrum suggested the presence of a number of species in solution, with some of the signals seemingly overlapped. A 2D TOCSY spectrum confirmed the presence of three independent spin systems (Figure S7). The ^{1}H NMR spectrum of **2** showed 11 separate peaks in the arene region of 5.1−6.2 ppm. Integration suggested that they corresponded to three species; two with three signals in a 2:1:2 ratio and one with five signals integrating for 1H each.

To characterize the three species present, chloride titrations for complexes **1** (6.5 mM Ru) and **2** (6.8 mM Ru) were followed by ^{1}H NMR spectroscopy in D_2O at 298 K. The

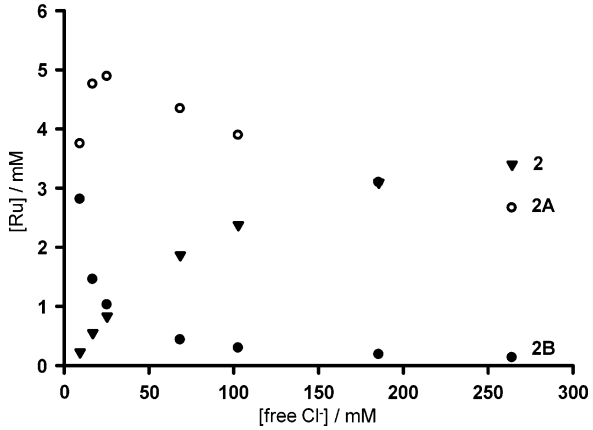

Figure 6. Plot of the concentration of ruthenium species versus the concentration of free chloride for $[(\eta^6{:}\eta^1\text{-}C_6H_5(CH_2)_2NH_2)RuCl_2]$ (**2**) on the basis of the integration of ^{1}H NMR peaks. The initial concentration of **2** was 6.8 mM. Symbols: (●) = $[(\eta^6{:}\eta^1\text{-}C_6H_5(CH_2)_2NH_2)Ru(H_2O)_2]^{2+}$ (**2B**), (○) = $[(\eta^6{:}\eta^1\text{-}C_6H_5(CH_2)_2NH_2)Ru(H_2O)Cl]^+$ (**2A**), and (▼) = $[(\eta^6{:}\eta^1\text{-}C_6H_5(CH_2)_2NH_2)RuCl_2]$ (**2**).

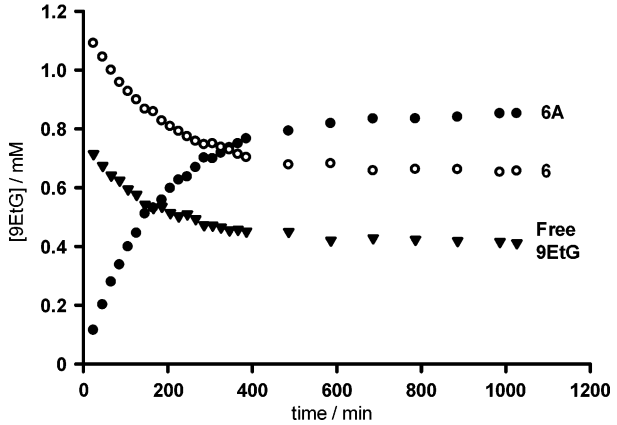

Figure 7. Plot of the concentration of 9EtG in the species versus time for the reaction of $[(\eta^6{:}\eta^1\text{-}C_6H_5(CH_2)_3NH_2)Ru(NO_3)_2]$ (**3**) (1.1 mM Ru) with 1.75 mol equiv of 9EtG at 298 K (pH 5.19 (start) − 6.22 (finish)). Symbols: (○) = $[(\eta^6{:}\eta^1\text{-}C_6H_5(CH_2)_3NH_2)Ru(9EtG)H_2O]^{2+}$ (**6**), (●) = $[(\eta^6{:}\eta^1\text{-}C_6H_5(CH_2)_3NH_2)Ru(9EtG)_2]^{2+}$ (**6A**), and (▼) = free 9EtG.

relative intensities of the three species present in solution changed with increasing concentrations of added chloride (Figures S8−S10). Integration of the arene proton peaks gave the relative proportions of the three species present in solution at each chloride concentration, as shown for complex **2** in Figure 6. The concentration of one adduct (**2B**) approached zero with increasing chloride concentration. The concentration of species **2A** appeared to reach a maximum at ca. 40 mM free chloride and decreased in the presence of further added chloride. The concentration of species **2** increased as the concentration of chloride increased. The variation in the concentrations of the three related ruthenium species with the concentration of free chloride for **1** was very similar to that for **2** (Figure S11). Equilibria appeared to be reached quickly, because spectra recorded after 20 min showed no changes when re-recorded after 22 h for solutions of **1** with $[Cl^-]_t$ = 12.9 or 273.1 mM and solutions of **2** with $[Cl^-]_t$ = 13.6 or 273.6 mM, where $[Cl^-]_t$ = total chloride concentration. This allowed the equilibrium constants to be determined, on the basis of the dependence shown in Chart 2. The equilibrium constants for **1** of K_1 = 145 and K_2 = 5.4 mM

Chart 2. Scheme for the Aquation (with Associated Equilibrium Constants K_1 and K_2) and Reaction of 9EtG with Tethered Ru^{II} Arene Complexes[a]

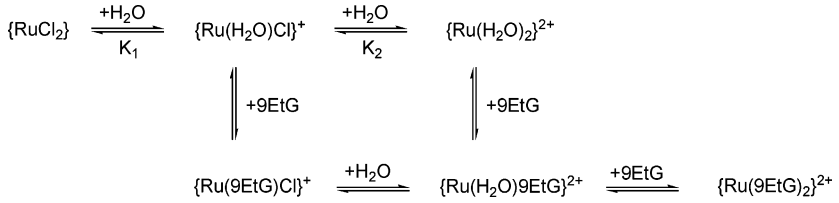

[a] Tethered ligands (η^6:η^1-$C_6H_5(CH_2)_nNH_2$), where n = 2 or 3, have been omitted in the formulas.

(Figure S12) are comparable with those of **2**, K_1 = 154 and K_2 = 6.5 mM, despite the poorer fit for the value of K_2 (Figure S13).

The ^{1}H NMR spectrum of a solution of [(η^1:η^6-$C_6H_5(CH_2)_3NH_2$)$Ru(NO_3)_2$] (**3**) in 90% H_2O/10% D_2O (9.4 mM) showed the presence of only one species at the initial pH 4.1. The observed ^{1}H NMR peaks have the same chemical shifts as those of the di-aqua adduct **1B** observed in an aqueous solution of the di-chlorido complex [(η^6:η^1-$C_6H_5(CH_2)_3NH_2$)-$RuCl_2$] (**1**), and the species is assumed to be [(η^1:η^6-$C_6H_5(CH_2)_3NH_2$)$Ru(H_2O)_2$]$(NO_3)_2$ (**3A**). A pH titration was followed by ^{1}H NMR in an attempt to determine the pK_a values associated with the coordinated aqua ligands. Raising the pH by the stepwise addition of NaOH led to precipitation at pH values as low as 4.8. At pH 7.7, the color of the solution was pale yellow. Peaks due to the initial di-aqua species began shifting to high field above pH 5.4. However, they had almost disappeared at pH 6.6, thus preventing the determination of the associated pK_a value(s) (Figure S14). During each experiment, the pH values measured before recording the spectrum were higher on average 0.2 pH units than those measured after. Three new species were present in solution, and the position of their signals did not shift between pH 5.0 to 11.0. When the pH was raised from 8.9 to 11.0, a fourth species appeared. Formation of these species was reversible, because on lowering the pH to 1.0, only the di-aqua species was observed to be present in solution. In addition, the precipitate redissolved. Upon raising the pH of an acidic solution of **3** directly to pH 10.1, the presence of peaks assignable to the four similar species was detected but in different proportions and no precipitate formed.

Reactions with Nucleobases. In a reaction of [(η^6:η^1-$C_6H_5(CH_2)_3NH_2$)$Ru(NO_3)_2$] (**3**) with 1.75 mol equiv of 9EtG in 90% H_2O/10% D_2O at pH 5.19, all of starting complex **3** appeared to have reacted by the time the first spectrum was recorded (24 min). H8 peaks for two new 9EtG adducts, a major one at 8.16 ppm (**6**) and a minor one at 8.25 ppm (**6A**), were observed in addition to the H8 peak for free 9EtG (7.82 ppm). Over time, the peaks corresponding to free 9EtG and **6** decreased in intensity, whereas those of **6A** increased in intensity. The product peaks can be assigned to [(η^6:η^1-$C_6H_5(CH_2)_3NH_2$)$Ru(9EtG)H_2O]^{2+}$ (**6**) and [(η^6:η^1-$C_6H_5(CH_2)_3$-NH_2)$Ru(9EtG)_2]^{2+}$ (**6A**) by the integration of the signals in the ^{1}H NMR spectra and by comparison with the shifts of the synthesized di-9EtG adduct [(η^6:η^1-$C_6H_5(CH_2)_3NH_2$)Ru-$(9EtG)_2$]$(NO_3)_{0.25}(PF_6)_{1.75}$ (**7**). Figure 7 shows a plot of the concentration of 9EtG in the adducts formed versus time. Formation of mono-9EtG adduct (**6**) is rapid and appears to have reached completion by the time the first spectrum was recorded. In contrast, formation of the di-9EtG adduct (**6A**) appeared to reach equilibrium after ca. 700 min and did not go to completion. With increasing time, a further, minor set of arene proton signals was noted, which did not appear to be assignable to a 9EtG adduct.

In a reaction of [(η^6:η^1-$C_6H_5(CH_2)_3NH_2$)$RuCl_2$] (**1**) with 2 mol equiv of 9EtG in the presence of chloride ($[Cl^-]_t$ = 21.7 mM), three sets of H8 peaks for 9EtG adducts were observed (8.16 ppm, two overlapped signals, **4** and **4A**, and 8.26 ppm (**4B**), in addition to an H8 peak for free 9EtG (7.82 ppm)).

In a reaction of [(η^6:η^1-$C_6H_5(CH_2)_2NH_2$)$RuCl_2$] (**2**) with 2 mol equiv of 9EtG in the presence of chloride ($[Cl^-]_t$ = 21.7 mM), complex **2** appeared to have completely reacted within 53 min, and [(η^6:η^1-$C_6H_5(CH_2)_2NH_2$)$Ru(H_2O)Cl]^+$ (**2A**) within 183 min. No di-aqua complex [(η^6:η^1-$C_6H_5(CH_2)_2$-NH_2)$Ru(H_2O)_2]^{2+}$ (**2B**) was detected by the time the first spectrum was recorded (32 min). Three new 9EtG H8 peaks (8.21, 8.26, and 8.28 ppm) were observed in addition to that for free 9EtG. Figure 8 shows a plot of the concentration of bound 9EtG in the adducts formed during the reaction versus time. Similar to the reaction with the dinitrato (di-aqua) complex (**3**), formation of the di-9EtG adduct (**5B**, H8 peak at 8.28 ppm) from dichloride complex **2** is time-dependent, and equilibrium was reached after ca. 22 h. The chemical shifts of the H8 peaks were compared to those observed in a separate experiment, in which the abstraction of chloride from **2** by silver nitrate in water was followed by the reaction with ca. 0.8 mol equiv of 9EtG. This suggested assignment of one of the two species as [(η^6:η^1-$C_6H_5(CH_2)_2NH_2$)Ru-$(9EtG)H_2O]^{2+}$ (**5A**, H8 peak at 8.26 ppm). Addition of NaCl and comparison of the chemical shifts of the new signals suggested the assignment of the other species as [(η^6:η^1-$C_6H_5(CH_2)_2NH_2$)$Ru(9EtG)Cl]^+$ (**5**, H8 peak at 8.21 ppm).

The ^{1}H NMR spectrum of [(η^6:η^1-$C_6H_5(CH_2)_3NH_2$)Ru-$(9EtG)_2$]$(NO_3)_{0.25}(PF_6)_{1.75}$ (**7**) in D_2O showed the 9EtG H8 peaks as a singlet at 8.25 ppm, a low-field shift of 0.43 ppm compared to free 9EtG. The broad tether-NH_2 signal, which was still detectable after 24 h, had shifted to low field from 3.92 for the di-aqua complex to 5.41 ppm (Figure 9A). Over the course of the experiment, the singlet at 8.25 ppm decreased in intensity, and two new H8 signals at 8.14 and 7.82 ppm, assignable to mono-9EtG adduct **7A** and free 9EtG respectively, increased in intensity. Equilibrium appeared to be reached after ca. 700 min. Part B of Figure 9 shows the plot of the concentration of **7**, **7A**, and free 9EtG versus time for the hydrolysis of **7**.

DNA Metalation Reactions. In reactions of [(η^6:η^1-$C_6H_5(CH_2)_3NH_2$)$Ru(NO_3)_2$] (**3**) with double-helical CT DNA,

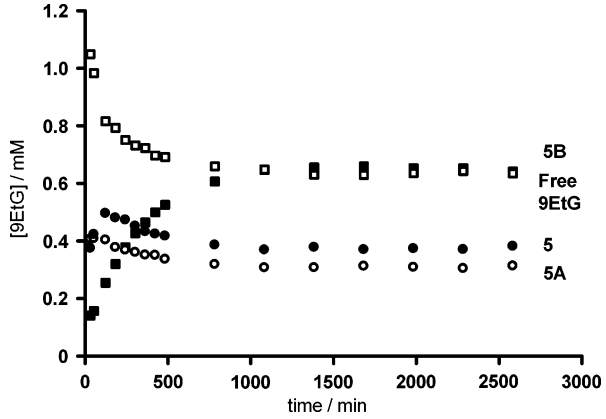

Figure 8. Plot of the concentration of 9EtG in the species formed during the reaction of $[(\eta^6{:}\eta^1\text{-}C_6H_5(CH_2)_2NH_2)RuCl_2]$ (**2**) (0.99 mM Ru) with 2.0 mol equiv of 9EtG at 298 K in the presence of chloride ($[Cl^-]_t$ = 21.7 mM, pH 6.08 (start) − 6.23 (finish)) versus time. Symbols: (●) = $[(\eta^6{:}\eta^1\text{-}C_6H_5(CH_2)_3NH_2)Ru(9EtG)Cl]^+$ (**5**), (○) = $[(\eta^6{:}\eta^1\text{-}C_6H_5(CH_2)_3NH_2)Ru(9EtG)H_2O]^{2+}$ (**5A**), (■) = $[(\eta^6{:}\eta^1\text{-}C_6H_5(CH_2)_3NH_2)Ru(9EtG)_2]^{2+}$ (**5B**), and (□) = free 9EtG.

the amount of ruthenium coordinated to DNA (r_b) increased with time. After ca. 20 min, all of the ruthenium from **3** present in the reaction mixture was bound to DNA. In this binding reaction, the time at which the binding reached 50% ($t_{50\%}$) was ca. 3 min. Importantly, the analytical methods that monitored the binding of ruthenium to DNA are not affected by any subsequent closure of monofunctional adducts to bifunctional lesions. The binding experiments indicated that such rutheniation reactions resulted in the coordination of all of the molecules of **3**, which made it possible to prepare easily and precisely samples of DNA modified by complex **3** at a preselected value of r_b.

DNA Transcription by RNA Polymerase In Vitro. In vitro RNA synthesis by RNA polymerases on DNA templates containing several types of bifunctional adducts of platinum complexes can be prematurely terminated at the level of or in the proximity of adducts.[29,39] On the other hand, monofunctional DNA adducts of several platinum complexes (such as [Pt(dien)Cl]Cl or $[PtCl(NH_3)_3]Cl$) are unable to terminate RNA synthesis.[29,39,43] Cutting of pSP73KB DNA[39] by *Nde*I and *Hpa*I restriction endonucleases yielded a 212 bp fragment (a substantial part of its nucleotide sequence is shown in part B of Figure S15). This fragment contained a T7 RNA polymerase promoter (in the upper strand close to its 3′ end (Figure S15)). The experiments were carried out using this linear DNA fragment, modified at r_b = 0.008 by **3** and for comparative purposes also by cisplatin, transplatin, or [Pt(dien)Cl]Cl, for RNA synthesis by T7 RNA polymerase (Figure S15; lanes **3**, cisPt, transPt and dienPt, respectively). RNA synthesis on the template modified by bifunctional platinum complexes (cisplatin or transplatin) yielded fragments of defined sizes, which indicates that RNA synthesis on these templates was prematurely terminated (Figure S15). On the other hand, no stop sites were produced by the adducts of the monofunctional platinum complex [Pt(dien)Cl]Cl and by **3**. These results are consistent with the view that **3** forms mainly monofunctional adducts on DNA.

(43) Brabec, V.; Boudny, V.; Balcarova, Z. *Biochemistry* **1994**, *33*, 1316−1322.

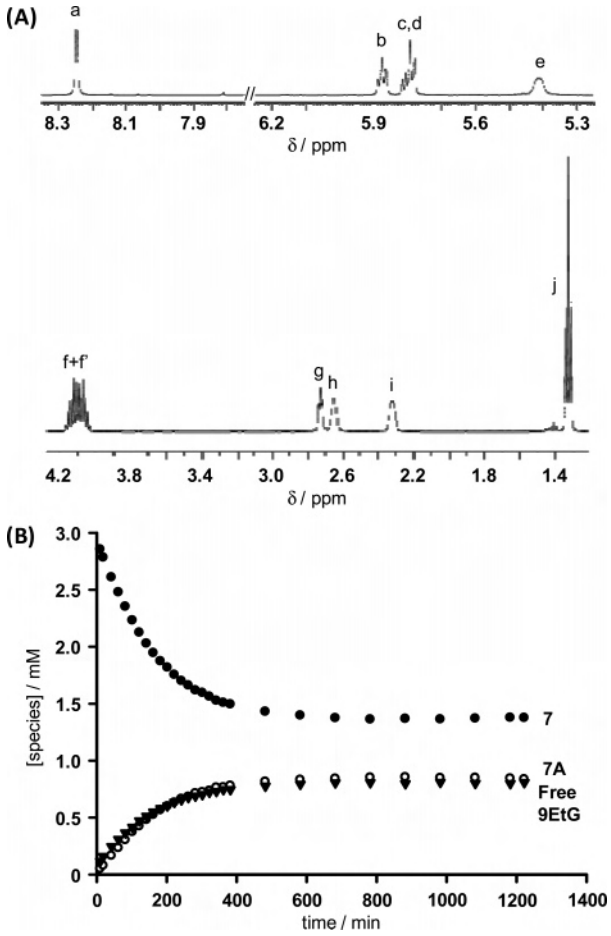

Figure 9. (A) ^{1}H NMR spectrum of $[(\eta^6{:}\eta^1\text{-}C_6H_5(CH_2)_3NH_2)Ru(9EtG)_2](NO_3)_{0.25}(PF_6)_{1.75}$ (**7**) in D_2O at 298 K (4.3 mM Ru) after dissolution at pH* 6.47. Assignments: a = H8; b, c, d = arene protons; e = NH_2 tether; f+f' = CH_2 (9EtG); g, h, i = $(CH_2)_3$ (tether); j = CH_3 (9EtG). (B) Plot of the concentration of species versus time for the hydrolysis of 9EtG from **7** (3.0 mM Ru) in D_2O at 298 K (pH* 6.67 (start) − 6.02 (finish)). Symbols: (●) = $[(\eta^6{:}\eta^1\text{-}C_6H_5(CH_2)_3NH_2)Ru(9EtG)_2]^{2+}$ (**7**), (○) = $[(\eta^6{:}\eta^1\text{-}C_6H_5(CH_2)_3NH_2)Ru(9EtG)H_2O]^{2+}$ (**7A**), and (▼) = free 9EtG.

DNA Interstrand Crosslinking Assay. Bifunctional compounds that bind strongly to DNA may form various types of interstrand and intrastrand cross-links. Therefore, we quantitated the interstrand cross-linking efficiency of **3** in linearized pSP73 plasmid (2464 bp). This plasmid DNA was linearized by *Eco*RI (*Eco*RI cuts only once within the pSP73 plasmid), 3′-end-labeled by [α-^{32}P] ATP, and modified by **3**. Cisplatin, which is known to form ca. 6% interstrand cross-links, was used for comparative purposes.[39] Upon electrophoresis, the 3′-end-labeled strands of linearized plasmid DNA containing no interstrand cross-links migrate as a 2464 base single strand, whereas the interstrand cross-linked strands migrate more slowly as a higher molecular mass species (Figure 10). This more slowly migrating band was observed when the DNA fragment was modified by cisplatin at r_b values as low as 0.0005, and its intensity increased with increasing levels of modification. For **3**, the slowly migrating band was observed only when the DNA fragment was modified at a considerably higher r_b value. The DNA interstrand cross-linking efficiency of **3** was almost independent of r_b and was only 0.2%. Thus, the DNA interstrand cross-linking efficiency of **3** was markedly lower

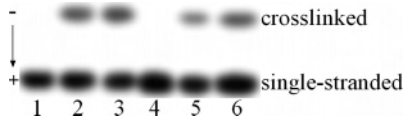

Figure 10. Formation of interstrand cross-links by [(η^6:η^1-$C_6H_5(CH_2)_3NH_2$)$Ru(NO_3)_2$] (**3**) and cisplatin in pSP73 plasmid that was linearized by *Eco*RI. Autoradiogram of denaturing 1% agarose gels of linearized DNA that was 3′-end labeled. The interstrand cross-linked DNA appears as the top bands (marked as cross-linked), which migrated on the gel more slowly than the single-stranded DNA (contained in the bottom bands and marked as single-stranded). The fragment was nonplatinated (control) (lane 1) or modified by cisplatin at $r_b = 5 \times 10^{-4}$, 1×10^{-3} (lanes 2, 3, respectively) or by **3** at $r_b = 5 \times 10^{-4}$, 1×10^{-3}, 1×10^{-2} (lanes 4−6, respectively).

Figure 11. Unwinding of supercoiled pSP73KB plasmid DNA by complex [(η^6:η^1-$C_6H_5(CH_2)_3NH_2$)$Ru(NO_3)_2$] (**3**). The plasmid was incubated with **3** for 24 h at 37 °C in 10 mM $NaClO_4$. Lanes: 1, 12 are controls consisting of nonmodified DNA ($r_b = 0$); 2 − $r_b = 0.01$; 3 − $r_b = 0.03$; 4 − $r_b = 0.05$; 5 − $r_b = 0.06$; 6 − $r_b = 0.07$; 7 − $r_b = 0.08$; 8 − $r_b = 0.09$; 9 − $r_b = 0.10$; 10 − $r_b = 0.15$; 11 − $r_b = 0.20$. The top bands correspond to nicked plasmid and the bottom bands to closed, negatively supercoiled plasmid.

than that of cisplatin (6%), consistent with the results of transription mapping (Figure S15), indicating that this complex forms mainly monofunctional lesions on DNA.

Unwinding of Negatively Supercoiled DNA. A compound that unwinds the DNA duplex reduces the number of supercoils in closed, negatively supercoiled DNA so that the negative superhelical density of closed circular DNA decreases. This decrease upon the binding of unwinding agents causes a decrease in the rate of migration through agarose gel, which makes it possible to observe and quantify the unwinding. Figure 11 shows electrophoresis gels in which increasing amounts of **3** have been bound to a mixture of relaxed and negatively supercoiled pSP73KB DNA. The unwinding angle is given by $\mu = 18\ \sigma/r_b(c)$, where σ is the superhelical density and $r_b(c)$ is the value of r_b at which the supercoiled and relaxed forms comigrate. Under the present experimental conditions, σ was calculated to be −0.04 on the basis of the data for cisplatin for which the $r_b(c)$ was determined in this study and $\mu = 13°$ was assumed. Using this approach, a DNA unwinding angle for **3** of $9 \pm 1°$ was determined.

Cytotoxicity. Complexes **1** and **2** were tested for cytotoxicity against the human ovarian cancer cell line A2780. The maximum test concentration employed was 100 μM, and at those concentrations, no significant inhibition of cell growth was observed. The complexes were thus deemed inactive.

Discussion

Synthesis and Characterization. The synthesis of tethered Ru^{II} arene complexes [(η^6:η^1-$C_6H_5(CH_2)_nNH_2$)$RuCl_2$] **1** ($n = 3$) and **2** ($n = 2$) was carried out via the thermal displacement of ethyl benzoate by a pendent arene. Arene exchange reactions are believed to proceed via the progressive dissociation of the arene ligand via η^6 to η^4 and η^2 coordination.[44] THF was added to the reaction mixture because of observations made by Bennett et al., who found that this shortened reaction times and gave higher yields for the synthesis of some phosphine-tethered complexes.[18c]

For **1** and **2**, the dramatic changes in the ^{1}H NMR shifts of the arene upon coordination to ruthenium and the associated 2:1:2 signal intensity pattern (cf. multiplet for uncoordinated arene) due to the equivalence of the two ortho and two meta protons, respectively, are the most significant evidence of coordination.[45] The pronounced low-field shift of the NH_2 signals by 1.4−2.0 ppm compared to the respective free ligands is characteristic of coordination.

X-ray Crystal Structures. The X-ray crystal structures of complexes [(η^6:η^1-$C_6H_5(CH_2)_3NH_2$)$RuCl_2$] (**1**) and [(η^6:η^1-$C_6H_5(CH_2)_2NH_2$)$RuCl_2$] (**2**) appear to be the first examples of di-chlorido Ru^{II} arene complexes containing a nitrogen-bound tether. Reported examples of neutral bifunctional complexes have mainly contained phosphorus-coordinated tethers.[18]

For phosphine-containing tethered complexes, the Ru−C(arene) bond lengths of compounds with three carbon atoms in the backbone are in the range of 2.16−2.27 Å, whereas those in **1** lie within the more narrow range of 2.161(9)−2.196(7) Å, together with a ca. 0.04−0.05 Å shorter Ru−centroid distance.[17,18b,c,46] This is similar to two-carbon tethers for which ranges of 2.15−2.28 Å have been reported. The Ru−centroid distance in **2** is ca. 0.06−0.08 Å shorter than in comparable analogues.[18a,f,21,23]

The structure of **2** appears to be more strained than that of **1**. The observed buckling of the coordinated arene in **2** seemingly is a consequence of the arene accommodating the strain exerted by the chelating tether. The added flexibility offered by three-atom tethered molecule **1** results in the arene adopting a more planar conformation. Strain is also reflected by a change in the Ru−C(arene)−C(tether) angle, which is 114.74° for **2** in contrast to 127.17° for **1**. Even though the crystal structures show the strain imposed on the arene by the tether in complex **2** with its 2-carbon tether, complexes **1** and **2** appear to have similar stability and hydrolysis behavior in aqueous solution. However, in donor organic solvents such as DMSO, complex **2** appears to undergo decomposition via the loss of arene, probably as a direct consequence of the strain.

There appears to be no previous report of a Ru^{II} arene complex containing two monodentate nitrate ligands such as those that are present in [(η^6:η^1-$C_6H_5(CH_2)_3NH_2$)$Ru(NO_3)_2$] (**3**). Nitrate generally is a weak ligand for ruthenium; however, there are other reported examples of dinitrato adducts including α-[$Ru^{II}(azpy)_2(NO_3)_2$],[47] where azpy = 2-(phenylazo)pyridine, and *cis*-[$Ru^{III}Cl(NO_3)_2$(pdma)NO],[48] where pdma = 1,2-phenylenebis(dimethylarsine), which both have shorter Ru−O bond lengths than **3**. Mono-nitrato

(44) Howell, J. A. S.; Ashford, N. F.; Dixon, D. T.; Kola, J. C. *Organometallics* **1991**, *10*, 1852−1864.
(45) Smith, P. D.; Gelbrich, T.; Hursthouse, M. B. *J. Organomet. Chem.* **2002**, *659*, 1−9.
(46) (a) Ghebreyessus, K. Y.; Nelson, J. H. *Organometallics* **2000**, *19*, 3387−3392. (b) Pinto, P.; Marconi, G.; Heinemann, F. W.; Zenneck, U. *Organometallics* **2004**, *23*, 374−380.
(47) Hotze, A. C. G.; Velders, A. H.; Ugozzoli, F.; Biagini-Cingi, M.; Manotti-Lanfredi, A. M.; Haasnoot, J. G.; Reedijk, J. *Inorg. Chem.* **2000**, *39*, 3838−3844.

Table 2. Ru−N7 Bond Lengths (Angstroms) of Ruthenium Complexes Containing Guanine Derivatives[m]

complex	Ru−N7
$[(\eta^6\text{-ben})Ru(9EtG)Cl_2]$	2.101(4)[a]
$[Ru_2(O_2CMe)_{1.82}(O_2CCF_3)_{0.18}(9EtG)_2(MeOH)_2]-(O_2CCF_3)_2.2MeOH.0.5Et_2O$	2.064(9), 2.078(9)[b]
$[(\eta^6\text{-ben})Ru(9EtG)_2H_2O](CF_3SO_3)_2$	2.124, 2.133[c]
$[(\eta^6\text{-ben})Ru(L\text{-ala})9EtG]Cl$	2.115(6), 2.112(7)[a]
$[(\eta^6\text{-bip})Ru(en)9EtG](PF_6)_2\cdot MeOH$	2.128(5)[d]
$[(\eta^6\text{-bip})Ru(en)Guo](PF_6)_2\cdot 3.75H_2O$	2.120(5)[d]
$[(\eta^6\text{-DHA})Ru(en)9EtG](PF_6)_2\cdot 2MeOH$	2.1173(15)[d]
$[(\eta^6\text{-THA})Ru(en)9EtG](PF_6)_2\cdot MeOH$	2.128(3)[d]
$\Delta\text{-}[Ru(bpy)_2(9MeG)_2](CF_3SO_3)_2$	2.122(5), 2.131(4)[e]
cis-$[Ru(bpy)_2(9EtG)Cl]Cl\cdot 1.5H_2O$	2.143(5)[f]
$[RuCl_3(9EtG)H_2O(DMSO)]$	2.148(3)[g]
$[(\eta^6\text{-bip})Ru(Et\text{-}en)9EtG](PF_6)_2$	2.123(5)[h]
$[(\eta^6\text{-}p\text{-cym})Ru(glycine)9EtG]PF_6$	2.136(3)[i]
$[(\eta^6\text{-}p\text{-cym})Ru(Ph_2acac)9EtG]CF_3SO_3\cdot 2tol$	2.126(3), 2.140(3)[j]
mer-$[RuCl_3(acv)DMSO(CH_3OH)]\cdot 0.5CH_3OH$	2.127(5)[k]
mer-$[RuCl_3(acv)DMSO(H_2O)]\cdot H_2O$	2.132(2)[k]
mer-$[RuCl_3(acv)DMSO(C_2H_5OH)]\cdot C_2H_5OH$	2.148(6)[l]

[a] Ref 14. [b] Ref 51a. [c] Ref 9. [d] Ref 13. [e] Ref 51b. [f] Ref 52a. [g] Ref 52b. [h] Ref 52d. [i] Ref 3. [j] Ref 52f. [k] Ref 52c. [l] Ref 52e. [m] Abbreviations: 9MeG = 9-methylguanine, acv = acyclovir, ben = benzene, bip = biphenyl, bpy = 2,2′-bipyridine, DHA = dihydroanthracene, en = ethylenediamine, Et-en = $Et(H)NCH_2CH_2NH_2$, Guo = guanosine, L-ala = deprotonated L-alanine, THA = tetrahydroanthracene.

ruthenium complexes are also known, including $[(\eta^5\text{-Cp})Ru(CO)(AsPh_3)NO_3]$,[49] where Cp = cyclopentadienyl, and $[(\eta^6\text{-}p\text{-cym})_2Ru_2(6,6'\text{-}Me_2dppz)(NO_3)_2]$,[+,50] where 6,6′-$Me_2$-dppzH = 2,2′-(1*H*-pyrazole-3,5-diyl)-bis(6-methylpyridine), which again have shorter Ru−O bond lengths than **3**.

The unrefined structure of $[(\eta^6{:}\eta^1\text{-}C_6H_5(CH_2)_3NH_2)Ru(9EtG)_2](NO_3)_2$ (**6A**) confirmed the CHN elemental analysis that suggests that the attempted counterion metathesis from NO_3^- to PF_6^- in $[(\eta^6{:}\eta^1\text{-}C_6H_5(CH_2)_3NH_2)Ru(9EtG)_2](NO_3)_{0.25}(PF_6)_{1.75}$ (**7**) was only partial, possibly due to the ability of nitrate to participate in hydrogen bond interactions with N1H and N2H (Figure S5).

Two features of the X-ray crystal structure of $[(\eta^6{:}\eta^1\text{-}C_6H_5(CH_2)_3NH_2)Ru(9EtG)_2](CF_3SO_3)_2\cdot H_2O$ (**8**·H_2O) are of particular interest. First, the significant difference between the two Ru−N7(9EtG) bond lengths of ca. 0.06 Å. Other Ru^{II} di-guanine derivative structures have more similar bond lengths (maximum difference of 0.015 Å) for the two coordinated guanines (Table 2).[9,14,51] Compared to reported di- and mono-guanine adducts of ruthenium,[3,13,14,52] the Ru−N7(9EtG) distance of 2.10 Å (Ru−N20, Table 1) found for one of the coordinated 9EtG molecules in the structure of **8**·H_2O appears to be one of the shortest. In contrast, the other Ru−N7(9EtG) bond length of 2.16 Å (Ru−N10, Table 1) in the structure of **8**·H_2O appears to be one of the longest reported. This difference in the Ru−N(9EtG) bond distances in **8**·H_2O could result from an electronic effect, where good overlap of the binding orbitals is not possible for the second molecule of 9EtG, or it could arise from steric hindrance around the metal center. Steric hindrance in the complex *cis*-$[Ru(bpy)_2(9MeG)_2]^{2+}$, where bpy = 2,2′-bipyridine and 9MeG = 9-methylguanine, resulting in hindered rotation of guanine, gives rise to two different H8 peaks for the coordinated 9MeG ligands.[51b] The ^1H NMR studies of $[(\eta^6{:}\eta^1\text{-}C_6H_5(CH_2)_3NH_2)Ru(9EtG)_2](NO_3)_{0.25}(PF_6)_{1.75}$ (**7**) in water show that the H8 signal for the two coordinated 9EtG ligands is a singlet integrating for 2H. This suggests that some degree of rotational freedom does exist for the two H8 protons. Interestingly, however, the CH_2 protons from the ethyl group of 9EtG in complex **7** give rise to two separate peaks (part A of Figure 9), which may be a consequence of rotational hindrance and slow exchange between conformations.

The formation of di-guanine adducts at metal centers have been particularly well studied for Pt^{II} complexes, mainly for cisplatin. For these systems, the relative orientation of the bases has received much attention.[53] They have been classified as head-to-head (HH) and head-to-tail (HT) orientations, with HH being energetically more favorable. In square-planar Pt^{II} systems, HH describes an orientation in which the two guanine bases are oriented in the same direction (i.e., the carbonyl groups are pointing in the same direction), and for HT, the bases are oriented in the opposite direction (i.e., the carbonyl groups point away from each other).

The second significant feature in the crystal structure of **8**·H_2O is the apparent directional influence of the tether amine group on the orientation of the coordinated 9EtG ligands via the formation of intramolecular hydrogen bonds. In the three reported ruthenium di-guanine derivative adducts, the orientation of the 9EtG and 9MeG ligands is HT.[9,51] Interestingly, in the structure of $[(\eta^6{:}\eta^1\text{-}C_6H_5(CH_2)_3NH_2)Ru(9EtG)_2](CF_3SO_3)_2\cdot H_2O$ (**8**·H_2O), the two 9EtG ligands are oriented toward each other, that is, they adopt an HH orientation. The influence of the amine group on this conformation is indicated by the angle between the plane defined by all of the arene carbons and that of C5 (where the tether is connected), Ru, and N(tether). This angle can be viewed as a measure of the outward swing of the tether. For the structures of three-atom tethered complexes $[(\eta^6{:}\eta^1\text{-}C_6H_5(CH_2)_3NH_2)RuCl_2]$ (**1**) and $[(\eta^6{:}\eta^1\text{-}C_6H_5(CH_2)_3NH_2)Ru(NO_3)_2]$ (**3**), this angle is close to 90°, whereas for **8**·H_2O it is 72.77°. This is presumably a consequence of the flexibility of the three-carbon tether, which enables the amine group to position itself so as to increase the hydrogen-bond

(48) Coe, B. J.; McDonald, C. I.; Beddoes, R. L. *Polyhedron* **1998**, *17*, 1997−2007.
(49) Cao, M.; Do, L. V.; Hoffman, N. W.; Kwan, M. L.; Little, J. K.; McGilvray, J. M.; Morris, C. B.; Söderberg, B. C.; Wierzbicki, A.; Cundari, T. R.; Lake, C. H.; Valente, E. J. *Organometallics* **2001**, *20*, 2270−2279.
(50) Catalano, V. J.; Craig, T. J. *Polyhedron* **2000**, *19*, 475−485.
(51) (a) Crawford, C. A.; Day, E. F.; Saharan, V. P.; Folting, K.; Huffman, J. C.; Dunbar, K. R.; Christou, G. *Chem. Commun.* **1996**, 1113−1114. (b) Zobi, F.; Hohl, M.; Zimmermann, I.; Alberto, R. *Inorg. Chem.* **2004**, *43*, 2771−2772.
(52) (a) van Vliet, P. M.; Haasnoot, J. G.; Reedijk, J. *Inorg. Chem.* **1994**, *33*, 1934−1939. (b) Price, C.; Shipman, M. A.; Gummerson, S. L.; Houlton, A.; Clegg, W.; Elsegood, M. R. J. *J. Chem. Soc., Dalton Trans.* **2001**, 353−354. (c) Turel, I.; Peèanac, M.; Golobiè, A.; Alessio, E.; Serli, B. *Eur. J. Inorg. Chem.* **2002**, 1928−1931. (d) Chen, H.; Parkinson, J. A.; Nováková, O.; Bella, J.; Wang, F.; Dawson, A.; Gould, R.; Parsons, S.; Brabec, V.; Sadler, P. J. *Proc. Natl. Acad. Sci. U.S.A.* **2003**, *100*, 14623−14628. (e) Turel, I.; Peèanac, M.; Golobiè, A.; Alessio, E.; Serli, B.; Bergamo, A.; Sava, G. *J. Inorg. Biochem.* **2004**, *98*, 393−401. (f) Melchart, M.; Habtemariam, A.; Parsons, S.; Sadler, P. J. *J. Inorg. Biochem.*, in press.
(53) Ano, S. O.; Kuklenyik, Z.; Marzilli, L. G. In *Cisplatin*; Lippert, B., Ed.; Verlag Helvetica Chimica Acta: Zürich, Switzerland, 1999; pp 247−291.

Table 3. Hydrolysis Equilibrium Constants for Metal Di-Chlorido Complexes

complex	K_1	K_2	I (M)	T (K)
cisplatin[a]	3.3−3.9	0.2−0.4	0.3	298−308
cisplatin[b]	6.4	0.3	0.1	298
cisplatin[c]	2.52	0.03	0.01	310
$[(\eta^6\text{-}p\text{-cym})Ru(pta)Cl_2]$[d]	0.03	107		298
$[(\eta^6{:}\eta^1\text{-}C_6H_5(CH_2)_3NH_2)RuCl_2]$ (**1**)	145	5.4		298
$[(\eta^6{:}\eta^1\text{-}C_6H_5(CH_2)_2NH_2)RuCl_2]$ (**2**)	154	6.5		298

[a] Ref 54a. [b] Ref 54b. [c] Ref 54c. [d] Ref 55; *p*-cym = para-cymene, pta = 1,3,5-triaza-7-phosphaadamantane.

interactions with both of the carbonyl groups. The carbonyl group with the strongest hydrogen bond to the tether amine protons belongs to the 9EtG ligand, which has the longest Ru−N7(9EtG) bond length. The observed low-field shift of ca. 1.5 ppm of the tether NH_2 protons in the ^{1}H NMR spectrum of **7** in D_2O is also characteristic of hydrogen-bonding interactions.

Aqueous Chemistry. Important features of the tethered complexes studied in this work are their aqueous solubility at millimolar concentrations and the stability of the tether chelate ring.

It is apparent that both coordinated chloride ligands in complexes **1** and **2** can undergo hydrolysis (Figures 6 and S8−S11). At extracellular chloride concentrations (ca. 0.1 M), the majority of the complexes could be expected to be present as the respective mono-aqua adducts, together with some di-chlorido complex, with negligible amounts of the di-aqua adduct. For the present tethered systems, aquation and loss of chloride are strongly favored, as is evident from the pronounced presence of monohydrolyzed species at chloride concentrations as high as 275 mM. Such a mono-aqua species would be expected to react readily with biomolecules.

With the exception of cisplatin,[54] there appear to be few reports of hydrolysis equilibrium constants for metal di-chlorido complexes. The equilibrium constants K_1 and K_2 determined for complexes **1** and **2** are considerably higher than those of cisplatin (Table 3); however, in all of the cases $K_2 < K_1$. Curiously, hydrolysis equilibrium constants reported for a phosphine-containing di-chlorido ruthenium arene complex[55] are very different from those reported here.[56] For both complexes **1** and **2**, the value for K_2 is comparable to that reported for the aquation of some monofunctional Ru^{II} arene complexes of the type $[(\eta^6\text{-arene})Ru(en)Cl]^+$.[57]

Dissolution of $[(\eta^6{:}\eta^1\text{-}C_6H_5(CH_2)_3NH_2)Ru(NO_3)_2]$ (**3**) in water produces signals for one species only, assumed to be the fully aquated complex. Similar complete aquation of the di-nitrato complex α-$[Ru(azpy)_2(NO_3)_2]$ in water has been reported.[47] The formation of four species over the range pH 4.1−11.0, the ^{1}H NMR signals of which did not shift over that pH range, and the reversible formation of the di-aqua species upon acidification suggest the involvement of hydroxides (or oxides) as bridging ligands, comparable to complexes such as $[((\eta^6\text{-}C_6H_6)Ru(\mu\text{-}OH))_4]^{4+}$ and $[((\eta^6\text{-}C_6H_6)Ru)_2(\mu\text{-}OH)_3]^+$, for which X-ray structures have been reported.[58,59] The proposed formation of hydroxo-bridged species appears to reflect a general feature exhibited by multifunctional metal complexes in aqueous solution. The facile formation of a precipitate at comparatively low pH values has also been observed for metallocenes. Kuo et al. have shown the existence of monomer−dimer equilibria for molybdocenes in water at pD 3.5.[60] In addition, Marks and Toney showed that titanocene can form an insoluble poly oxo- and hydroxo-bridged species in water.[61] Similarly, the formation of a poly oxo-bridged species by the Ru^{III} complex NAMI-A occurs in water at low pH values.[62]

Adducts with Nucleobases. Reaction of $[(\eta^6{:}\eta^1\text{-}C_6H_5(CH_2)_3NH_2)Ru(NO_3)_2]$ (**3**) with 9EtG in water results in the rapid formation (<24 min at 298 K) of the mono-9EtG adduct $[(\eta^6{:}\eta^1\text{-}C_6H_5(CH_2)_3NH_2)Ru(9EtG)H_2O]^{2+}$ (**6**) and the comparatively slow and incomplete formation of the di-9EtG adduct $[(\eta^6{:}\eta^1\text{-}C_6H_5(CH_2)_3NH_2)Ru(9EtG)_2]^{2+}$ (**6A**). This, together with the results of the reverse reaction, the displacement of 9EtG from $[(\eta^6{:}\eta^1\text{-}C_6H_5(CH_2)_3NH_2)Ru(9EtG)_2]^{2+}$ (**7**) by water, suggests weak binding of the second 9EtG molecule. Interestingly, the 9EtG−N7 bond lengths in the structure of **8**·H_2O appear to correlate with the relatively strong binding of one 9EtG and the relatively weak binding of the other 9EtG ligand, when compared to other reported structures (Table 2).

It was of interest to study the reactivity of both $[(\eta^6{:}\eta^1\text{-}C_6H_5(CH_2)_3NH_2)RuCl_2]$ (**1**) and $[(\eta^6{:}\eta^1\text{-}C_6H_5(CH_2)_2NH_2)RuCl_2]$ (**2**) with 9EtG in the presence of ca. 22 mM chloride, comparable to cytoplasmic $[Cl^-]$.[63] The equilibria were reached after ca. 22 h, significantly longer than in the chloride-free reaction of $[(\eta^6{:}\eta^1\text{-}C_6H_5(CH_2)_3NH_2)Ru(NO_3)_2]$ (**3**). Because in the chloride titration of complex **2**, the major species present at ca. 20 mM $[Cl^-]_f$ was the mono-aqua mono-chlorido adduct **2A**, the reaction of **2** with 9EtG presumably proceeds via the initial formation of $[(\eta^6$:

(54) (a) Reishus, J. W.; Martin, D. S. *J. Am. Chem. Soc.* **1961**, *83*, 2457−2462. (b) Hindmarsh, K.; House, D. A.; Turnbull, M. M. *Inorg. Chim. Acta* **1997**, *257*, 11−18. (c) Kankia, B.; Funck, T.; Marky, L. A. *J. Solution Chem.* **1999**, *28*, 1249−1261.

(55) Scolaro, C.; Bergamo, A.; Brescacin, L.; Delfino, R.; Cocchietto, M.; Laurenczy, G.; Geldbach, T. J.; Sava, G.; Dyson, P. J. *J. Med. Chem.* **2005**, *48*, 4161−4171.

(56) In the context of hydrolysis of bifunctional complexes, loss of a negatively-charged chloride ligand from a neutral complex (mono-aquation) would be expected to be more favorable than further loss of chloride from a positively-charged complex (i.e., second aquation step), reflected by $K_2 < K_1$. For the bifunctional ruthenium arene complex $[(\eta^6\text{-}p\text{-cymene})Ru(pta)Cl_2]$, where pta = 1,3,5-triaza-7-phosphaadamantane, simultaneous hydrolysis of both chloride ligands was proposed.[55] However, in subsequent ^{1}H NMR solution studies the presence of only the mono-aqua species was detected (A. Dorcier et al., *Organometallics* **2006**, *25*, 4090−4096), that is, preferential mono-aquation, which appears not to conform to the proposed hydrolysis pathway and thus the reported equilibrium constants.

(57) Wang, F.; Chen, H.; Parsons, S.; Oswald, I. D. H.; Davidson, J. E.; Sadler, P. J. *Chem.—Eur. J.* **2003**, *9*, 5810−5820.

(58) Gould, R. O.; Jones, C. L.; Robertson, D. R.; Stephenson, T. A. *J. Chem. Soc., Chem. Comm.* **1977**, 222−223.

(59) Arthur, T.; Robertson, D. R.; Tocher, D. A.; Stephenson, T. A. *J. Organomet. Chem.* **1981**, *208*, 389−400.

(60) Balzarek, C.; Weakley, T. J. R.; Kuo, L. Y.; Tyler, D. R. *Organometallics* **2000**, *19*, 2927−2931.

(61) Toney, J. H.; Marks, T. J. *J. Am. Chem. Soc.* **1985**, *107*, 947−953.

(62) Bouma, M.; Nuijen, B.; Jansen, M. T.; Sava, G.; Flaibani, A.; Bult, A.; Beijnen, J. H. *Int. J. Pharm.* **2000**, *248*, 239−246.

(63) Jennerwein, M.; Andrews, P. A. *Drug Metab. Dispos.* **1995**, *23*, 178−184.

η^1-$C_6H_5(CH_2)_2NH_2$)Ru(9EtG)Cl]$^+$ (**5**) via the displacement of water from **2A**. Successive, possibly fast, hydrolysis of the chloride from **5** would result in an increase in the presence of [(η^6:η^1-$C_6H_5(CH_2)_2NH_2$)Ru(9EtG)H_2O]$^{2+}$ (**5A**), which can then further react with another molecule of 9EtG.

On the basis of the results of the binding experiments, a scheme for the reaction of tethered Ru^{II} arene complexes with 9EtG in the presence of chloride can be proposed (Chart 2). Formation of the di-9EtG adduct is inhibited by competition from aquation. In addition, the presence of chloride not only inhibits the formation of the di-9EtG adduct further, but also slows down the formation of mono-9EtG adducts, compared to reactions of the di-aqua species.

DNA Binding. The values of DNA unwinding angles are affected by the nature of the ligands in the coordination sphere of the metal and the stereochemistry at the metal center. Previous systematic work[41,64] has revealed that, for instance, Pt^{II} compounds fall into different classes, according to their DNA binding modes. It has been shown that Pt^{II} compounds with the smallest unwinding angles (6°) are those that can bind DNA only monofunctionally ([Pt(dien)Cl]Cl or [$Pt(NH_3)_3$Cl]Cl). In contrast, platinum compounds that bind in a bifunctional manner unwind DNA by 10−13°. Examples include cisplatin, its trans isomer, and bifunctional polynuclear complexes. The observation that [(η^6:η^1-$C_6H_5(CH_2)_3NH_2$)Ru(NO_3)$_2$] (**3**), which unwound DNA by ∼9°, can be grouped together with monofunctional Pt^{II} compounds that unwind DNA only slightly is readily understood in terms of an adduct structure in which **3** is preferentially coordinated to DNA in a monodentate manner. This monofunctional adduct, however, is formed readily, because the reactivity of **3** with 9EtG and double-helical CT DNA, both in terms of the rate and the extent of binding, was found to be very similar.

Cytotoxicity. Complexes **1** and **2** were found to not exhibit cytotoxic activity against the human ovarian cell line A2780 at a significant concentration (IC_{50} > 100 μM). This is in agreement with other tested ruthenium arene compounds with two potentially reactive sites, containing pyridine and phosphine ligands, which showed only negligible cytotoxicity against some cancer cell lines.[12,55] The results of this work suggest that, under cell-testing conditions, complexes **1** and **2** would be expected to be present to a large extent as the mono-aquated complex in the extracellular medium ([Cl^-] ca. 0.1 M). Thus, the complexes might react with components of the cell culture medium and become deactivated. In addition, the possible formation of hydroxo-bridged species at physiological pH would also contribute toward the deactivation of these complexes. Such factors could limit the comparatively strong, monofunctional binding of, for example, complex **3** to DNA and result in little cytotoxicty. Furthermore, the observed lack of interstrand cross-link formation on DNA by complex **3** could lead to deactivation via the second vacant binding site on the ruthenium center, for example by protein binding, which could weaken the Ru−DNA bond (cf. hydrolysis of 9EtG from **7**) and lead to the removal of ruthenium from DNA. This could explain why other ruthenium arene complexes of the type [(η^6-arene)-Ru(en)Cl]$^+$, which form stable monofunctional adducts with, for example DNA, are considerably cytotoxic[3] whereas the tethered complexes are not.

Conclusions

The bifunctional di-chlorido, nitrogen-tethered Ru^{II} arene complexes [(η^6:η^1-$C_6H_5(CH_2)_3NH_2$)$RuCl_2$] (**1**) and [(η^6:η^1-$C_6H_5(CH_2)_2NH_2$)$RuCl_2$] (**2**) were synthesized. These complexes are water-soluble and undergo rapid aquation to form mono- and di-aqua adducts. Loss of one chloride is strongly favored, and anation was not complete even in the presence of a large excess of chloride (ca. 275 mM). Hydroxo-bridged species appear to be formed from the di-aqua adduct over a range of pH 5.4−11.0. Thus, in aqueous biological media, these complexes may be deactivated by reactions with biomolecules or by the formation of unreactive bridged species.

The reactivity of these bifunctional tethered Ru^{II} arene complexes toward 9-ethylguanine was investigated. In the absence of chloride, rapid binding of one 9EtG was observed followed by the slow formation of a di-9EtG adduct, over a period of ca. 10 h. Formation of di-9EtG adducts appears to be suppressed by the presence of chloride. The X-ray crystal structure of the di-9EtG adduct [(η^6:η^1-$C_6H_5(CH_2)_3NH_2$)Ru-(9EtG)$_2$](CF_3SO_3)$_2$·H_2O (**8**·H_2O) revealed an unusual HH orientation of the two bases, with the formation of intramolecular hydrogen bonds between the tether NH_2 group and C6O(9EtG). Furthermore, the X-ray structure is consistent with the strong binding of one 9EtG ligand and the weak binding of the other, as observed in aqueous solution. Biophysical measurements on plasmid DNA showed only monofunctional binding of [(η^6:η^1-$C_6H_5(CH_2)_2NH_2$)Ru(NO_3)$_2$] (**3**), again consistent with the weak binding of a second nucleobase observed by ^{1}H NMR solution studies. Overall, the (bio)chemical reactivity of the bifunctional tethered complexes **1** and **2** appears not to be compatible with anticancer activity. However, the low toxicity of these complexes might be a useful feature, tuneable for other biological applications.

Acknowledgment. We thank Oncosense Ltd for support for P.J.S., the Grant Agency of the Czech Republic (Grants 305/05/2030 and 203/06/1239), and the Academy of Sciences of the Czech Republic (Grants 1QS500040581 and KAN200200651) for support for V.B., COST D20/D39 for stimulating discussions, Emily Jones and Daniel Cole (Oncosense Ltd) for carrying out the cytotoxicity tests, and Mr. Juraj Bella, at the University of Edinburgh, for NMR advice and assistance.

Supporting Information Available: Details of synthesis of ethylbenzoate dimer, synthetic routes as Charts S1 and S2, crystallographic data in Tables S1−S5, NMR spectra, X-ray structures, and a gel showing restriction mapping as Figures S1−S15.

IC700799W

(64) (a) Zaludova, R.; Zakovska, A.; Kasparkova, J.; Balcarova, Z.; Vrana, O.; Coluccia, M.; Natile, G.; Brabec, V. *Mol. Pharmacol.* **1997**, *52*, 354−361. (b) Balcarova, Z.; Kasparkova, J.; Zakovska, A.; Novakova, O.; Sivo, M. F.; Natile, G.; Brabec, V. *Mol. Pharmacol.* **1998**, *53*, 846−855. (c) Brabec, V.; Kasparkova, J.; Vrana, O.; Novakova, O.; Cox, J. W.; Qu, Y.; Farrell, N. *Biochemistry* **1999**, *38*, 6781−6790. (d) Kasparkova, J.; Marini, V.; Najajreh, Y.; Gibson, D.; Brabec, V. *Biochemistry* **2003**, *42*, 6321−6332.